

Radial growth decline in a tropical Andean treeline in Bolivia

Rose Oelkers^{1,2}, Laia Andreu-Hayles^{1,3,4}, Rosanne D'Arrigo¹, Hung T. T. Nguyen², Arturo Pacheco Solana^{2,5}, Milagros Rodriguez-Caton^{2,6}, M. Eugenia Ferrero^{6,11}, Ernesto Tejedor⁷, Alfredo F. Fuentes^{8,9}, Carla Maldonado^{8,9}, Daniel Ruiz-Carrascal¹⁰

¹Lamont-Doherty Earth Observatory of Columbia University, Palisades, NY 10964, USA
²Department of Earth Science and Environmental Change, University of Illinois Urbana-Champaign, Urbana, IL, USA
³Ecological and Forestry Applications Research Center (CREAF), Bellaterra, Spain
⁴Catalan Institution for Research and Advanced Studies (ICREA), Barcelona, Spain
⁵Department of Land, Environment, Agriculture and Forestry (TeSAF), University of Padua, 35020 Legnaro, Italy
⁶Instituto Argentino de Nivología, Glaciología y Cs. Ambientales (IANIGLA), CONICET Mendoza, Argentina
⁷Department of Geology, National Museum of Natural Sciences-Spanish National Research Council (MNCN-CSIC), Madrid, Spain
⁸Herbario Nacional de Bolivia, Instituto de Ecología, Carrera de Biología, Facultad de Ciencias Puras y Naturales, Universidad Mayor de San Andrés, La Paz, Bolivia
⁹Latin America Department, Science & Conservation Division, Missouri Botanical Garden, St. Louis, MO, USA
¹⁰Innovation and Technological Development Directorate, Universidad EAFIT, Medellín, Colombia
¹¹Laboratorio de Dendrocronología, Universidad Continental, Huancayo, Peru

Correspondence to: Rose Oelkers roelkers@ldeo.columbia.edu; rc019@illinois.edu

Abstract. The impacts of rising temperatures in tropical treeline ecosystems remains understudied. Here we report on a remarkable decline in the radial growth of *Polylepis pepei* BB.Simpson, a tropical tree species that grows in a monospecific forest at the elevational treeline in the Andes-Amazon ecotone of Bolivia. Using dendrochronological methods we developed an annually resolved tree-ring width chronology spanning from 1850 to 2018 C.E. To our knowledge this is the longest record of annual tree-growth (169 yrs) for this species. This chronology revealed a significant ($p = 0.01$) radial growth decline in *P. pepei* after 1997, which was also observed in other high-elevation *Polylepis* forests of tropical South America ($> 17^\circ$ S; 4600 m a.s.l.). Between 1960-2015, *P. pepei* RW was mostly regulated by prior-year minimum temperature and mean precipitation variability during the wet season (–November–March). RW-climate correlations suggest the observed growth decline at this tropical treeline is likely due to temperature driven moisture stresses. Smaller ring-width was associated with drier and warmer conditions in the forest while wetter and cooler conditions led to enhanced growth in the following year. Between 1960-2015, minimum temperature significantly increased during the wet season, while precipitation decreased. These climate trends observed in our study region in the Madidi National Park may indicate a reduction in moisture convergence and transport to higher elevations where our forest is located. If temperature continues to rise at current rates, one of the highest-elevation tree species on the globe, *P. pepei*, could face severe consequences.

- Formatted ... [1]
- Deleted: Solana¹
- Deleted: Caton¹
- Formatted: Font: 12 pt
- Formatted ... [2]
- Deleted: Affiliations¹
- Formatted ... [5]
- Formatted ... [4]
- Deleted: Department
- Formatted ... [6]
- Deleted: Ecological
- Formatted ... [7]
- Deleted: Catalan
- Formatted ... [8]
- Deleted: Department
- Formatted ... [9]
- Deleted: Instituto
- Formatted ... [10]
- Deleted: Department
- Formatted ... [11]
- Deleted: Herbario
- Formatted ... [12]
- Deleted: Latin
- Formatted ... [13]
- Deleted: Innovation
- Deleted: .
- Formatted ... [14]
- Formatted ... [15]
- Formatted ... [16]
- Formatted ... [17]
- Deleted: Relative to research efforts in higher latitudes, t ... [18]
- Deleted: climate shifts
- Deleted: the
- Deleted: Little is known about the tree growth dynamics & ... [22]
- Formatted ... [19]
- Formatted ... [20]
- Formatted ... [21]
- Deleted: This work provides insights into the past and his ... [24]
- Formatted ... [23]

250 **1 Introduction**

251 The stability of tropical Andean treeline communities under global warming has become of great concern due to observed shifts
252 in forest composition, distribution and increased tree mortality in recent decades (Cuesta et al., 2020; Feeley et al., 2012, 2011;
253 Macek et al., 2009; Young and León, 2006). In South America, forests found near the mountain peaks in the Andes Mountains
254 are often referred to as ‘treeline’ or high mountain areas in literature (Hock et al., 2019; Körner, 2012; Young and León, 2006)
255 and the term used herein is used to describe the upper range limits of the tree species found in the region. Plot studies in the
256 Peruvian Andes-Amazon found that the position of Andean timberline (i.e. elevational limit of closed-canopy forests) is limited
257 by seed dispersal (Rehm and Feeley, 2013). Dendrochronology has been widely used to evaluate annual growth variability and
258 long-term climate response of treeline forests in the northern Hemisphere (Büntgen et al., 2022; D’Arrigo et al., 1999;
259 MacDonald et al., 2007). However, tropical tree-ring studies in South America (~8°N-24°S), are noticeably scarce in
260 comparison to higher latitude regions (Andreu-Hayles et al., 2023; Groenendijk et al., 2025; Quesada-Román et al., 2022).
261 Still, some relevant studies have provided key understanding of climate-growth response of high elevation forests in the
262 tropical Andes as described below.

263
264 A study from the Peruvian puna (upper Andes) presented the first tree-ring chronology of *Escallonia myrtilloides* L.phil.
265 (Requena-Rojas et al., 2021), a species often found at tropical treeline (Zapata, 2013), in which the authors showed radial
266 growth is positively correlated to precipitation, and negatively correlated to temperature variability in this region. In the central
267 Andes of Peru, Requena-Rojas et al. (2020) analyzed the tree rings from three *Polylepis* species, and found these trees are
268 slow-growing and sensitive to both current-year temperature and prior year precipitation changes. In subtropical regions, prior-
269 year moisture availability was the dominant limiting factor for *Polylepis tarapacana* Phil. treelines in Argentina, based on
270 RW-climate correlations spanning 1934-1980 (Morales et al. 2004) On the other hand, the growth of several tropical montane
271 species in northern Argentina appears to be regulated only by temperature at the upper elevations of an altitudinal gradient
272 (Ferrero et al., 2013). Although seedling recruitment of *Nothofagus pumilio* is driven by temperature variability, the rate of
273 seedling establishment was limited by overall moisture conditions in Patagonia (Sruur et al., 2018, 2016). Yet, there was a radial
274 growth decline in *Nothofagus pumilio* at a Chilean treeline site, where precipitation had increased (Álvarez et al., 2015),
275 possibly suggesting a non-linear growth response of these forests to climate.

276
277 Here we describe a tropical treeline site of *Polylepis pepeii* BB.Simpson (Simpson, 1979), growing high elevations (3800 -
278 4000 m.a.s.l.) in the Andes-Amazon corridor of Bolivia in South America. This site is located at upper forested limit of
279 Bolivia’s Madidi National Park (MNP), a hotspot for biodiversity just east of the Cordillera Real in the Andes Temperature
280 and humidity gradients shape unique ecotones in the MNP including diverse seasonally dry forests near the Tuichi River (~850
281 m.a.s.l.) and humid monospecific forests at Andean treeline (~4400 m.a.s.l.)—The hydroclimate of the MNP (and Andes-
282 Amazon) is primarily influenced by the South American Summer Monsoon (SASM), which peaks in the tropics during austral

Moved (insertion) [1]

Moved (insertion) [2]

Formatted: English (US)

Formatted: Font color: Auto, English (US)

Deleted: Temperature-limited treelines have been well studied in dendrochronology. In the Northern Hemisphere (NH), shifts in latitudinal and elevational treeline have been associated with the effects of global warming (Flynn et al.,

Moved down [5]: 2020).

Moved up [1]: 2020; Feeley et al., 2012, 2011; Macek et al., 2009; Young and León, 2006).

Deleted: For instance, shifts in tree-ring width (RW) have been linked to upward recruitment and ecotonal shifts in forests in the Pyrenees (Batllori and Gutiérrez, 2008). In the European Alps (Paulsen et al., 2000) treeline advances may be associated with radial growth response to minimum temperature thresholds and interannual climate variations overall. A tree-ring network of dominant conifer species from the French Alps found a common radial growth signal since 1930, which may be attributed to (... [25]

Deleted: Overall, several studies across Eurasia found inc (... [26]

Deleted: Conversely, some treeline sites in boreal North A (... [27]

Deleted: The stability of tropical treelines and high-moun (... [28]

Deleted: A recent report for the IPCC (Hock et al., 2019) (... [29]

Formatted: Font color: Auto

Formatted: Font color: Black

Formatted: English (US)

Formatted: Font color: Auto, English (US)

Moved up [2]: In South America, forests found near the

Deleted: Plot studies in the Peruvian Andes-Amazon four (... [30]

Deleted: in the tropical Andes

Deleted: related

Deleted: Also in

Deleted: a genus that dominates the treeline forests of So (... [31]

Deleted: Morales et al. (2004) reported that changes in (... [32]

Deleted: growth in

Deleted: .

Deleted: in

Deleted: forests

Deleted: , the growth of different species

Deleted: In the temperate *Nothofagus pumilio* (Poepp. & (... [33]

Deleted: facilitates tree recruitment in northern and south (... [34]

Deleted: can be strongly modulated by the interaction bet (... [35]

Formatted: Font color: Custom Color(70,70,70)

Moved (insertion) [7]

380 summer (December-February). Inter-annual to decadal sea surface temperature sea-surface temperature (SST) conditions in
381 the Pacific and Atlantic Oceans also impact climate in the region (Paegle and Mo, 2002; Vuille et al., 2000). Originating in
382 the tropical Pacific, the El Niño Southern Oscillation (ENSO) system is the dominant mode of annual to decadal hydroclimate
383 variability in South America and indeed the globe (e.g. Garreaud, 2009; Vera et al., 2006; Vuille et al., 2000). ENSO-related
384 anomalies SST anomalies have contributed to extreme weather events in South America such as seasonal drought, flooding,
385 and other geohazards (Vera et al., 2006; Vuille et al., 2000). Tree-ring width and oxygen isotopes have recorded these extreme
386 events at treeline *P. tarapacana* in the central tropical Andes and provided year-to-year to centennial records of ENSO
387 variability overall(Christie et al., 2009; Crispin-DelaCruz et al., 2022; Rodriguez-Caton et al., 2022) Currently there is no
388 information on the impacts of such ENSO-related climate extremes on *Polylepis pepeï* tree-rings, or for treeline sites within
389 the MNP.

391 The geographic range of *Polylepis pepeï* (family Rosaceae; common name “Kenua” or “Queñoa”) spans from central Bolivia
392 to northern Peru (Simpson, 1979) between 3550-4800 m.a.s.l. (Espinoza and Kessler, 2022). Tree-ring studies in Bolivian and
393 Peru have shown *P. pepeï* can reach significant age (>135 years) and the RW can be sensitive to prior and current-year climate
394 variability (Jomelli et al., 2012; Roig et al., 2001).The wide dispersion of leaves along the branches in *P. pepeï* and its long
395 fruit distinguish this species from other *Polylepis* spp. The genus name *Polylepis* is derived from the Greek words ‘many
396 layers’, describing multiple layers of compressed thin-bark sheets, a functional trait that allows these trees to survive freezing
397 air temperatures. This species is also adapted to cold soil temperatures in the eastern cordillera of the Andes. Ecological studies
398 of *P. pepeï* sites between 3800–4300 m.a.s.l. in Peru (Kessler et al., 2014) and Bolivia (Hoch and Körner, 2005) recorded (>
399 5cm) soil temperatures ranging from 3-5°C during the wet season.

401 Like much of the treeline species across the Andes-Amazon, *P. pepeï* is under threat of shifting temperature regimes and
402 human impacts on the ecosystem. Some studies predict the germination and spatial distribution of treeline *Polylepis spp* in the
403 Andes is projected to decrease as vapor pressure deficits, temperatures, and overall aridity increase (Cuyckens et al., 2016;
404 López et al., 2022). Southwest of our *P. pepeï* site, in the central Andes of southern Peru ice proxy data indicated recent
405 surface warming in the tropics that appears unprecedented in 5000 years (Thompson et al., 2006). In November 2009
406 temperatures were so warm that a catastrophic glacial lake outburst flood eliminated roads, livestock, and structures in the
407 small community of Keara Bolivia (< 3800 m.a.s.l. (Hoffmann and Weggenmann, 2013). In the MNP, there is evidence of a
408 temperature-induced migration (i.e. thermophilization) of mid-elevation tree species towards Andes ecotones caused by
409 increased of tree mortality near the treeline (Farfan-Rios et al., 2025).

411 Humans also play a role in modifying the forested landscape near the MNP. Illegal mining and logging activities in low-
412 elevation forests (<1200 m.a.s.l.) have deteriorated forest structure and health, with increasing loss of forest cover in recent
413 years (Finer and Mamani, 2023). Prior to the designation of Madidi as a National Park in 1995, large swaths of economically-

Moved (insertion) [8]

Moved (insertion) [9]

Moved (insertion) [10]

Moved (insertion) [11]

Deleted: Here we describe a tropical treeline site for the species *Polylepis pepeï* BB.Simpson (Simpson, 1979), growing high elevations (3700 m.a.s.l-4000 m.a.s.l.)

Moved up [7]: in the Andes-Amazon corridor of Bolivia in South America.

Moved up [8]: Originating in the tropical Pacific, the El Niño Southern Oscillation (ENSO) system is the dominant mode of annual to decadal hydroclimate variability in South America and indeed the globe (e.g. Garreaud, 2009; Vera et al., 2006; Vuille et al., 2000).

Moved (insertion) [12]

Deleted: This site is located at upper forested limit of Bolivia’s Madidi National Park (MNP), a hotspot for biodiversity within the vast Amazon forest, located just east of the Cordillera Real in tropical Andes. The hydroclimate of the Amazon-Andes ecotone in the MNP and broader region is primarily influenced by the South American Summer Monsoon (SASM), which peaks in the tropics during austral summer (December-February). Interannual to decadal sea surface temperature (SST) conditions in the Pacific and Atlantic Oceans (Paegle and Mo, 2002; Vuille et al., 2000) also impact climate in the region.

Deleted: ENSO varies between warmer (El Niño) and cooler (La Niña) phases (Ropelewski and Halpert, 1987), and both extremes substantially impact precipitation and temperature conditions over tropical South America. The Atlantic sector also plays a major role in South American climate, as defined, for example, by tropical North Atlantic (TNA) and tropical South Atlantic (TSA) indices, which supply zonal moisture transport across tropical South America (Enfield et al., 1999; Good et al., 2008).

Complex topography in the Andean foothills contributes to a variety of microclimatic conditions and variable controls on tree growth, complicating efforts to directly compare large-scale patterns of climate and tree-ring variability (typically RW) within or between species in a stand. This complexity, and the forest dynamics of the humid Amazon Basin drive gradients in temperature and humidity, shaping patterns of vegetation (Fuentes, 2005), e.g. between the lower, drier forests near the Tuichi River (~850 m.a.s.l.) and the upper Andean treeline (~4400 m.a.s.l.).

Moved (insertion) [13]

Formatted: Font color: Auto

Moved (insertion) [14]

452 valuable trees along riverbanks (e.g. *Amburana cearensis* Smith) were harvested for timber (Macía, 2008). Today, *P. pepeii* is
453 at great risk of endangerment due to habitat loss related to fires and land conversion for cattle ranching or religious practices
454 (Espinoza and Kessler, 2022; Kessler et al., 2014). These losses of primary forests have severe implications for carbon storage
455 capacity, ecosystem function, and land stability, all critical factors for the survival of native inhabitants. Herein, efforts were
456 made to minimize potential impacts of land use and disturbance in field sampling, but ecosystem disturbances in certain regions
457 of the MNP were nevertheless observed. Since this ecotone is facing a rapidly changing environment due to climate and
458 human-related disturbances, high resolution tree-ring records at this treeline may offer valuable insight on past and current
459 growth responses.

461 At present, only two tree-ring studies have been published for the MNP: one for *Juglans boliviana* (C.DC.) Dode (14°40' S,
462 68°41' W; 1300 m.a.s.l.) in Oelkers et al. (2023) and another by Andreu-Hayles et al. (2015), the latter confirming the formation
463 of annual rings in a *Pseudomedia rigida* (Klotzsch & H.Karst.) Cuatrec. cross-section (14°33'S, 68°49'W; 1000 m.a.s.l.). The
464 *Polylepis pepeii* site investigated for this study is found between ~~3800~~-4400 m.a.s.l. in the western MNP (14°40'-14°43'S;
465 69°04'-69°06'W). Located near the small settlement of Keara, the vegetation is characterized as Alto-Andino Yungueño (Upper
466 Andean Yungas) forest (Navarro et al., 2010) with a seasonally humid climate. This study area was chosen in part because
467 inventory plots already exist at this location, established by botanists from the National Herbarium in La Paz (Bolivia) and the
468 Missouri Botanical Garden (USA). Our specific objective are: i.) to generate a new RW chronology for *P. pepeii*, ii.) to identify
469 the climate variables (e.g. mean temperature, precipitation, drought), that are the most limiting for annual growth and iii.) to
470 assess the impacts of extreme climate events on the RW variations.

472 2 Materials and Methods

473 2.1 Site description and climatology

474 Our study site is located in northwestern Bolivia (Fig. 1A), where two locations were visited in October 2012 and July 2019
475 to extract samples of *P. pepeii* trees at altitudinal treeline in Keara (Fig. 1C, D). Two to four core samples were extracted from
476 living trees using 2-threaded increment borers (5 mm in diameter). Cross sections of recently dead trees were sliced using a
477 gas-powered chainsaw or a standard saw-tooth blade. In 2019, diameter at breast height (DBH; ~1.2 m) was measured for the
478 trees at the same level that core samples were extracted.

479
480 The 2012 collection was from an open-canopy south-facing forest (3795-~~4100~~ m.a.s.l.), while the 2019 collection was
481 primarily focused in a closed-canopy west-facing stand in a high-elevation valley called Waca-cocha (named after a nearby
482 lagoon; 4000-4400 m.a.s.l.; Fig. 1D). Both sites feature seasonally humid, upper-montane forests, with persistent mist that
483 evaporates during the day. The sites were largely monospecific, dominated by fragmented patches of *P. pepeii* and small

Moved (insertion) [15]

Moved up [9]: (Espinoza and Kessler, 2022).

Moved up [10]: (Jomelli et al., 2012; Roig et al., 2001).

Deleted: There is thus much need for additional dendrochronological research in this area, particularly at treeline and the greater forested ecotone between the Andes and Amazon Basin.¶

¶ In the MNP, mid-elevation woody species typically endure greater annual temperature and elevational ranges than lowland or highland species, based on monitoring studies (Montaño-Centellas et al., 2024). Species composition in the tropical Andes is often related to latitude and elevation as well (Malizia et al., 2020). Despite temperature-driven increases in tree mortality and species migration between 500-3600 m.a.s.l., above-ground biomass increased between 2003-2014 in eastern Andean forests (Duque et al., 2021). This increase was largely driven by intact old-growth forests, for which 30% of the regrowth was attributed to large-sized trees after disturbances. These studies provide information about spatial features of species distribution and abundance and carbon storage in the Andes-Amazon and specifically the MNP. The results herein add an additional, complementary dataset on annual radial growth patterns and climate sensitivity of an Andean treeline site not previously available.¶

¶ The geographic range of *Polylepis pepeii* (family Rosaceae; ... [36]

Deleted: The genus name *Polylepis* is derived from the G... [37]

Deleted: ¶ ... [38]

Deleted: 3700~

Deleted: In the following sections we

Deleted: those

Deleted: or

Deleted:)

Deleted: related trends and

Deleted: . In so doing we demonstrate, through ... [39]

Deleted: methods

Moved down [16]: 2023).

Deleted: Climate data¶ ... [40]

Deleted: Monthly and seasonal climate data were based on ... [41]

Deleted: Fig. 1 shows the location of the study sites in Ke ... [42]

Deleted: west of the small community in Keara

Deleted: 4000

Deleted: ; Fig. 1C), which was originally surveyed during ... [43]

Deleted: made southeast of Keara

Deleted: remote,

Deleted: near the sampling site) (

Deleted: These

Deleted: are

598 ~~numbers~~ of *Gynoxys compressissima* Cuatrec. trees. ~~Based on field observations in July 2019, the foliage of *P. pepeii* may be~~
599 ~~considered evergreen and the bark~~ consists of thick layers of compressed flakes that are red and brown in color, characteristic
600 of the genus ([Appendix A: Fig. A2A](#)). The trees are shrublike, with twisted (and at times, multiple) stems.

601
602 The climatology of the study site (1960-2015 Figs. 1B, A1) shows a distinct wet season from October-April and a dry season
603 from June-August (1960-2015; Fig. 1B). The wet season is defined by heavy rainfall (~1900 mm in January; Pre), and warmer
604 mean (6°; Tavg) and maximum temperatures (Tmax: 12-14.7°C). In contrast, the dry season is characterized by low
605 precipitation (65 to 115 mm per month) and extremely cold temperatures (minimum temperature range -7.1 to -8.3°C; Fig A1).
606 Consistent with these patterns the mean diurnal temperature range (the difference between Tmax and Tmin, DTR; Fig A1 B.)
607 is smallest during the peak wet season (12.1 to 16.9°C) due to warmer minimum temperatures (~0°C), and highest during the
608 drier months. Wet-season precipitation and temperature (Oct-Apr) was significantly and negatively correlated between 1960-
609 2015 ($r=-0.27$, $p=0.05$) indicating wetter months at this site are typically associated with cooler temperatures, while no
610 significant correlations were found during the dry season.

611 2.2 Climate data

612 In this study, we used local precipitation data, and gridded temperature products to generate monthly climate indices near
613 Keara (1960-2015; Fig. 1B). Daily precipitation from the Italaque station in Bolivia (15.48°S, 69.03°W, 3500 m.a.s.l.) was
614 gap filled and homogenized to generate a continuous monthly timeseries (Pre) from 1960-2015 following procedures described
615 in [Huerta et al. \(2025a\)](#) and the 'redprecc' package in *R* ([Huerta et al. 2025b](#)). Raw (daily) precipitation data for Italaque
616 (1978-2005) and nearby stations (~1945-2015, non-continuous) can be obtained from the DECADE dataset ([Hunziker et al.](#)
617 [2018](#)), which were originally sourced from the National Meteorology and Hydrology Service of Boliva (SENAMHI;
618 <https://senamhi.gob.bo/index.php>). Monthly mean (Tavg), minimum (Tmin), maximum (Tmax) temperature data was obtained
619 from the Climatic research Unit TS 4.08 (CRU; 0.5° resolution; [Harris et al. 2020](#)). ~~In addition, we also used CRU monthly~~
620 ~~diurnal temperature range (DTR; 0.5° resolution; 1901-2015), which represents the difference between Tmax and Tmin, to~~
621 ~~evaluate temperature variability in the region. The monthly climatology (1960-2015) and long-term variability of DTR (and~~
622 ~~Tmax and Tmin; 1901-2015) can be found in Appendix A Figs. A1 and A4 (see section 2.5 for more details). Satellite-derived~~
623 ~~rainfall data from the Climate Hazards Infrared Precipitation with Station group V2.0 (CHIRPS, accessed 2025; [Funk et al.](#)~~
624 ~~2015) was used for spatial precipitation analyses (see Section 2.5). Although CHIRPS v2.0 is limited to observations after~~
625 ~~1981, it has a higher spatial resolution (0.05°) than CRU precipitation (0.5°), which can be more effective for spatial climate-~~
626 ~~growth analyses in regions with complex topography such as our site in the Andes-Amazon.~~

627
628 In August 2011 (one year before the 2012 sampling campaign), HOBO® temperature and relative humidity data loggers
629 (<https://www.onsetcomp.com/>) were installed near the *P. pepeii* trees at 14°40'S 69°06'W (4158 m.a.s.l.) and data was recorded
630 hourly from 1 September 2011 to 2 September 2014. New HOBO sensors were installed in 2021 and collected during fieldwork

Deleted: amounts

Deleted: As noted

Deleted: bark

Deleted: pepeii

Deleted: 2A

Deleted: ¶

Core samples were extracted from living trees using 2-threaded increment borers (5 mm in diameter). Cross sections of dead trees were sliced using a gas-powered chainsaw or standard saw-tooth blade. Stem diameter was measured at the same level that core samples were extracted (at breast height ~1.2 m).

Formatted: Font color: Black

Deleted: during the 2012 visit to Keara

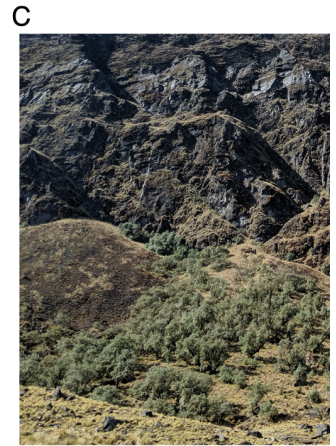
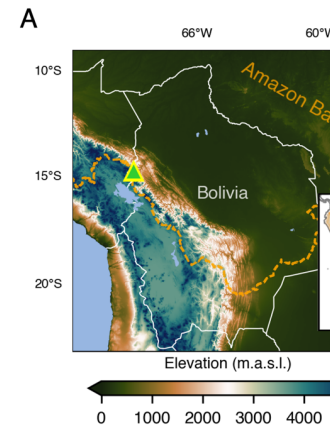
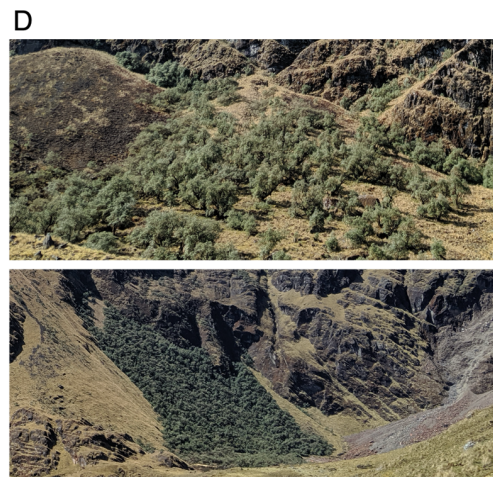
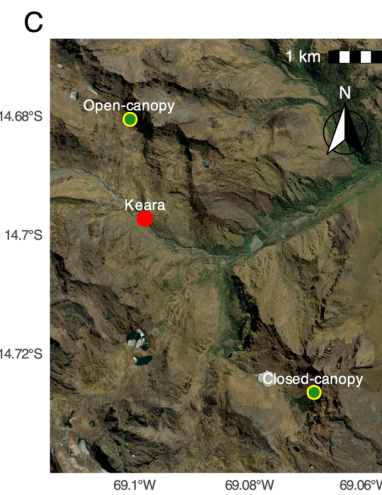
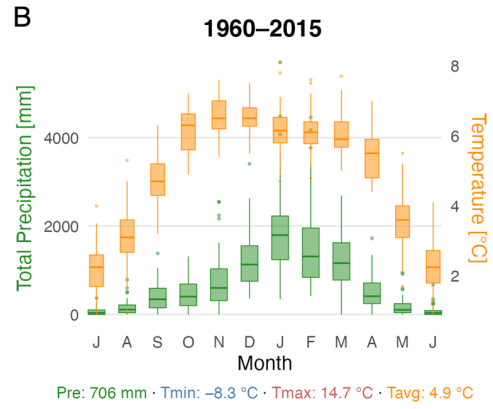
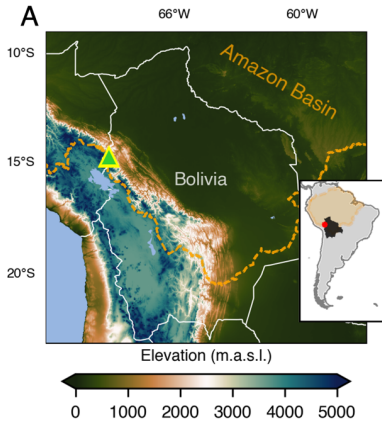
Deleted: the

644 in 2023. Unfortunately, the 2021 system batteries failed within 9 months of the launch, and data was limited to only 20
645 September 2021 to 23 May 2022. Daily minimum, maximum and mean temperature and relative humidity were calculated
646 from 20 September to 23 May (245 days) for the 2011-2012, 2012- 2013, 2013-2014 and 2021-2022 periods, (see Appendix A
647 Fig. A3. Kernel density estimates were used to generate and compare probability distributions among the daily time series,
648 Nonparametric Kolmogorov-Smirnov (KS) tests (Kolmogorov, 1933; Smirnov, 1948) were conducted to determine the
649 significance of the mean difference between the daily timeseries. Kernel density and KS tests were conducted using seaborn
650 (Waskom, 2021) and SciPy (Virtanen et al., 2020) packages in *python*.

651

Deleted: .

Deleted: and nonparametric



- Deleted:
- Deleted: near Keara
- Deleted: .
- Formatted: Font: 10 pt
- Formatted: Font: 10 pt
- Deleted: Monthly climatology (1981-2019) for Keara based on minimum and maximum
- Formatted: Font: 10 pt
- Deleted: from CRU 4.07
- Deleted: from CHIRPS
- Formatted: Font: 10 pt
- Formatted
- Deleted: data. Photos
- Formatted: Font: 10 pt

654 **Figure 1: (A) Location of *Polylepis* site in the Eastern Cordillera of the Andes-Amazon ecotone in Bolivia. The orange**
 655 **dotted line (and orange shading in the inset map) represent the spatial limits of the Amazon Basin. The elevation map**
 656 **was generated using the “ETOPO-1” model (<https://www.ncei.noaa.gov/products/etopo-global-relief-model>); (B) The**
 657 **monthly distribution of mean temperature and total precipitation (1960-2015) in Keara was generated using the**
 658 **nearest temperature CRU gridpoint (14.75°S, 69.5°W) and reconstructed precipitation from the Italaque station**
 659 **(15.48°S, 69.03°W). The average temperature (Tavg), mean precipitation (Pre), and range of minimum and maximum**
 660 **temperatures (Tmin, Tmax) for the study period are included. (C) Aerial view of the sampling locations near the**
 661 **temperatures (Tmin, Tmax) for the study period are included.**

678 **community of Keara and (D) photos of open-canopy and closed canopy forest patches sampled at altitudinal treeline in**
679 **Bolivia's MNP (~3700-4400 m.a.s.l.). The basemap in (C) was obtained through opensource ESRI images.**

680 2.3 Wood processing and anatomical analyses

681 Wood samples were shipped to the Lamont-Doherty Earth Observatory (LDEO) in NY, USA for dendrochronological analysis.
682 Cores and cross sections were finely sanded up to 1000 grit using an orbital sander and manually polished with microfiber
683 paper. Most samples had surficial color differences within the stem, mainly reflecting transitions between the heartwood
684 (**functional xylem near the pith, darker color**) and sapwood (the active **xylem** beyond the cambium layer, **lighter color**).

685
686 *P. pepei* is an angiosperm with diffuse porous wood anatomy, which is typically harder to date than 'ring porous' wood, due
687 to less distinct boundaries between the latewood of the prior year and the earlywood of the current year (Fig. A2). **To aid in**
688 **identifying anatomical properties in the wood, histological (micro) cuts were performed according to techniques described**
689 **in von Arx et al. (2016) using a WSL Core microtome (<https://www.wsl.ch/en/services-produkte/microtomes/>).** *P. pepei* tree
690 rings feature large, semicircular vessel elements in the earlywood that taper tangentially in size towards the transition to
691 latewood, which has thicker, fiber-like tracheid cells (Fig. A2 B).

692 2.4 Tree-ring chronology development

693 Tree rings **from 51 *P. pepei* samples from 28 living and 3 dead trees (31 trees total) were** dated visually using standard
694 dendrochronological techniques (Stokes and Smiley, 1968). RW was measured digitally using the *CooRecorder* image analysis
695 program (Cybis Elektronik, 2010) **and statistically crossdated using the program COFECHA (Holmes, 1983) and dplR package**
696 **in R (Bunn, 2008). To independently confirm annual periodicity of the growth rings, radiocarbon dating** was conducted on a
697 cross-section sample (SP20X; Fig. A2) collected in 2019 in the closed-canopy forest. Individual growth rings associated with
698 the years 1957, 1958, 1962, 1963, 1964, 1965, 1971, and 1972 were sliced, extracted for cellulose, and processed for modern
699 radiocarbon analyses. All radiocarbon measurements were compared to the monthly SH $\Delta^{14}\text{C}$ radiocarbon curve (1950-2019
700 C.E.) from the designated atmospheric Zones 1-2 and 3 (SH Zone 1-2; Hua et al., 2022). **Further details on the radiocarbon**
701 **analyses and earlier iterations of the Keara RW chronology can be found in the Appendix (Fig. A2 C).**

702
703 Once final calendar dates were assigned to the tree-ring samples, the Schulman convention (Schulman, 1956), which assigns
704 each ring date to the year growth began, was applied. Individual RW time series were detrended conservatively with age-
705 dependent cubic splines (initial spline stiffness of 60 yrs) (Cook and Peters, 1981; Melvin, 2004). **Standardized indices were**
706 **generated** by taking the ratio of the fitted and observed RW values of detrended time series and combined using a robust Tukey
707 bi-weight mean to produce a dimensionless 'standard' RW chronology (Cook et al., 1990). **For the residual chronology,**
708 **autocorrelation was removed from the series using autoregressive modelling determined by the Akaike Information Criterion**
709 **(Akaike, 1974). The final RW chronologies (standard and residual) represent the entire *P. pepei* RW network (2012 and 2019**

Deleted: (KEPP; C)

Deleted: (SP; D)

Deleted: which were

Formatted: Font: 10 pt

Formatted: Font: 10 pt

Formatted: Font: 10 pt

Formatted: Font: 10 pt

Deleted: 4300

Deleted:)

Formatted: Font: 10 pt

Formatted: Font: 10 pt

Deleted: variable ...ransitions between the heartwood (functional xylem near the pith, darker color, middle to interior of the st... [45]

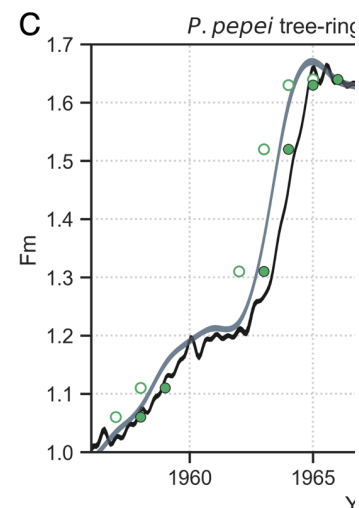
Moved down [17]: To aid in identifying anatomical properties in the wood, histological (micro) cuts were performed according to

Deleted: (2016) using a WSL Core microtome (<https://www.wsl.ch/en/services-produkte/microtomes/>). *P.*

Moved (insertion) [17]

Deleted: .

Deleted: 2B; Roig et al. 2001



Deleted:

Deleted: measured and... dated visually using standard dendrochronological techniques (Stokes and Smiley, 1968)

851 tree samples) and thus variance stabilization was applied to account for temporal changes in sample depth (Frank et al., 2006).
852 The standard RW chronology was used for RW-climate correlation analyses, and the residual chronology was used for i.)
853 identification of small or large outliers in the chronology (top 5th and 95th percentiles) and ii.) analyses of the growth response
854 of *P. pepei* to extreme ENSO events (see section 2.6).

855
856 The subsample signal strength (SSS) calculation was used to estimate the minimum sample size required to maintain a growth
857 common signal (Wigley et al., 1984). SSS considers the number of cores per tree, the number of individual trees and the mean
858 interseries correlation among RW series to determine how well the available samples reflect the growth signal of the population
859 (i.e. site). An SSS value of 0.85 (or better) is a common threshold in dendrochronology and represents the period when sample
860 size is adequate and the common RW signal is robust (see discussions Buras et al., (2017) and Wigley et al. (1984) for more
861 details). The Pettit's (1979) changepoint detection test was applied to the raw (radial) RW chronology to detect the timing of
862 recent trends in growth. Significance of the RW trend after the changepoint ($p < 0.05$) was determined by using the non-
863 parametric Mann-Kendall test on the estimated Sen's slope (Sen, 1968). Changepoint analyses was conducted using the 'trend'
864 package in R (Pohlert, 2016).

865 2.5 Climate-growth analyses

866 To explore the climate sensitivity of *Polylepis pepei* at the treeline, we correlated annual RW to monthly temperature and
867 precipitation for the period 1960-2015. Monthly temperature data (Tavg, Tmin, Tmax) was from the nearest CRU gridpoint to
868 our site: 14.75°S, 69.25°W, while monthly precipitation (Pre) was obtained from local station data (see section 2.2). Monthly
869 Pearson correlations (r) were computed with the stationary bootstrap method implemented with the boot package in R. This
870 technique resamples contiguous blocks of data ($n = 1000$) at varying block size to preserve autocorrelation and quantify the
871 uncertainty of the RW-climate relationship (see Politis & Romano 1994). Significance of the climate-growth relationship was
872 inferred from the two-tailed 95% confidence intervals (i.e., 95% CI excludes zero). Due to the covariance between temperature
873 and precipitation in this region, we used bootstrapped partial correlations (r_p) to evaluate the independent effect of one variable
874 on RW (e.g. temperature), while controlling for the other (e.g. precipitation). Following methods of Meko et al. (2011), partial
875 correlation coefficients for RW-temperature were obtained by: i.) first performing a linear regression between RW and
876 precipitation and ii.) calculating bootstrapped correlations between temperature and the residuals from this regression. The
877 results represent the portion of RW variability not explained by precipitation. Thus, partial correlations show the distinct
878 relationship between RW and temperature while controlling for the influence of precipitation.

879
880 Spatial correlations were used to assess the extent of the temperature (Tmax and Tmin) and precipitation signals of the RW
881 within tropical south America. Seasonal climate windows selected for the spatial analyses were inferred from the monthly
882 climate-growth relationships. Spatial correlations with precipitation were conducted using CHIRPS between 1981-2015 (see
883 section 2.2). Otherwise, all monthly and (seasonal) spatial correlation analyses (RW vs. climate) were between 1960-2015.

Deleted: i.)

Deleted: 5

Deleted: 95

Deleted: for

Deleted: declining population-size through time

Deleted: is often used for climate reconstruction purposes

Deleted:).

Deleted: used on

Deleted: and standard

Deleted: and significance ($p < 0.05$)

Deleted: growth shifts

Deleted: a

Deleted: .

Deleted: analysis

Deleted: Temperature

Deleted: signal in *P. pepei* growth rings

To determine the relationships between the RW timeseries, temperature, and

Deleted: , monthly and seasonal

Formatted: Font color: Black

Deleted: via bootstrapped correlations using the 'treeclim'

Deleted: (Zang and Biondi, 2015).

Formatted: Font: Not Italic

Deleted: the 'seascorr' function (Meko et al., 2011)

Deleted: significance

Deleted: the correlation of

Deleted: without the covariance with

Deleted: , and the other way around.

Deleted: with

Deleted: are

Deleted: , partial

Deleted: , which

Deleted: tree-growth

Deleted: temperatures without

Deleted: Spatial correlations (significance $p < 0.05$) were also computed to assess the extent of the temperature and precipitation signals of the RW records across space for the most significant season for each tree species.

Field significance was assessed using a binomial test (e.g. the probability n number of grid-cell correlations were significant by chance (raw $p < 0.05$) due to the high number of comparisons; see: Livezey & Chen, 1983).

Linear trends in the local (seasonal) climate (1960-2015) were assessed using the Sen's slope estimator (section 2.4), and significance was evaluated using Mann Kendall tests. Slopes were reported as the average change in climate in units per decade (Fig. A4) Annual and seasonal (October-April; June-August) trends of diurnal temperature anomalies (DTR) were also evaluated for the same period. Additionally, monthly anomalies of Tmin, and Tmax were calculated relative to the 1901-2015 CRU baseline (full temporal extent of CRU data) to illustrate long-term temperature variability during the wet and dry season (Fig. A5 BC).

2.6 Superposed Epoch Analysis

ENSO varies between warmer (El Niño) and cooler (La Niña) SST phases (Ropelewski and Halpert, 1987) in the Pacific Ocean, and both extremes substantially impact precipitation and temperature conditions over tropical South America. To investigate the effects of extreme ENSO events on tree growth, Superposed Epoch Analysis (SEA) was performed on the residual RW timeseries (Fig. 2D) using the method originally described by Haurwitz and Brier (1981) and modified by Rao et al. (2019). SEA is widely used to statistically determine whether the effects of episodic events (e.g. extreme climate events) on a response variable (in this case RW) are statistically significant or due to random noise. The Rao method uses 1000 random-sample double bootstrapping to quantify the RW response at the time of the event ($Jag = 0$) and several years after (in this case four years).

We analyzed twenty-six years of RW based on the top-ranked December-February (DJF) El Niño and La Niña events ($n=13$ each) listed by the National Oceanic and Atmospheric Administration's Physical Science Laboratory (NOAA-PSL: <https://psl.noaa.gov/enso/>). These ranked DJF years are determined by NOAA-PSL with the multivariate ENSO indices (MEI; 1871-2024). MEI reflects the principal components, or dominant modes, of the entire tropical Pacific ENSO domain (30°N-30°S, 100E°-70°W) rather than any one region (e.g. Niño 3.4) and integrates observations of sea level pressure (SLP), SSTs, meridional (north-south) wind, and outgoing longwave radiation (see Wolter and Timlin, 2011). Extreme years are defined by Pacific SST anomalies during DJF, coincidentally when ENSO is phase-locked with the peak monsoon season (Rasmusson and Carpenter, 1982). Annual Pre (station data; 1960-2015) and CRU precipitation and Tavg (nearest gridpoint 1901-2018) were plotted to determine the average climate during years of known ENSO-DJF events near Keara. The list of DJF- ENSO-events obtained from NOAA-PSL are included in Appendix Table A1.

Formatted: Heading 2

Moved up [18]: 2.6 Superposed Epoch Analysis*

Deleted: climate

Deleted: , including the potential impact of ENSO

Deleted:

Deleted: 3B

Deleted: ENSO

Deleted: t

Deleted: 4

Deleted: Table 1 lists the years of known precipitation anomalies in tropical South America connected to El Niño (warmer) or La Niña (cooler) conditions in the Pacific Ocean.

Deleted: The twelve

Deleted: years

Deleted:) based on

Deleted: extended

Deleted: index

Deleted: .ext) (

Deleted: -2005) and MEIv2.ext (1979-

Deleted:) were used. This bimonthly dataset is based on

Deleted: dominant modes, or

Deleted: sea surface temperature (SST),

Deleted: MEIv2.ext) (

Deleted: The ranking of extreme ENSO

Deleted: is mainly

Deleted:

Deleted: El Niño

... [50]

3 Results

3.1 Growth decline in a *P. pepei* tree-ring chronology

The *P. pepei* RW chronology from the MNP treeline spans from 1850-2018 and consists of 51 tree-ring samples (31 trees) from open and closed-canopy forests near Keara (Table 1; Fig. 2). Radiocarbon and standard dendrochronological methods confirmed the growth rings are annual and reflect high frequency patterns of high and low growth through time (Figs. 2A, C, D). Site metadata and chronology statistics for the *P. pepei* network are summarized in Table 1.

Site	Location (elevation)	<i>n</i> trees (<i>n</i> samples)	Mean age [yrs]	Timespan	Mean RW Correlation	Mean DBH [cm]
Open-canopy forest (south-facing)	14°40'S 69°06'W (3795-4100 m.a.s.l.)	16 living 2 dead (33)	89	1850-2018	0.53	24 cm (<i>n</i> =6 trees) *
Closed-canopy forest (west-facing)	14°43'S 69°04'W (4000-4400 m.a.s.l.)	12 living 1 dead tree (18)	101	1871-2018	0.44	31 cm
Full network (mean Raw, standard, residual chronologies)	-	31 (51)	93	1850-2018	0.50	30 cm

Table 1. Summary of *P. pepei* tree-ring sample location, age, sample size, and mean correlation of RW timeseries per site. *DBH information is only from the samples collected in 2019 which included 6 trees from the open-canopy forest and 13 trees from the closed-canopy site. The final RW chronologies represent the entire collection of *P. pepei* samples in Keara obtained in both 2012 and 2019.

Due to extreme suppression in radial growth (Fig. 2B), only one or two cores per tree (out of three total) were able to be cross-dated and used for the final RW datasets. A recent decrease in radial growth was observed in samples from both the open-canopy (18 trees) and closed canopy (13 trees) sites (Fig. 2A). The entire Keara *P. pepei* network (mean raw RW; Fig. 2A) has been declining steadily since the 1960s, especially after 1996 ($p=0.01$), with a less pronounced trend in the standard RW series (Fig. 2AC).

Despite difficulties with crossdating due to suppressed tree-rings, the entire network shared a coherency in the RW patterns with a mean inter-series correlation of $r = 0.50$ for the 1850-2018 period ($n = 51$ samples, 31 trees). The SSS metric indicated the common growth signal was particularly robust (SSS > 0.85) between 1900-2018 when the sample size was greater than 17 (Fig. 2C; average age of the trees 93 yrs). The average radial growth rate between 1850-2018 was 1.04 mm yr^{-1} . DBH measurements in 2019 (6 trees in the open canopy and 13 in the closed-canopy site), confirmed these trees were slow-growing with stem diameters ranging from 10 cm to 54 cm (mean DBH 30 cm).

Deleted: northern Bolivia (max elevation 4400 m.a.s.l.)

Deleted: 1868

Deleted: is shown in Figure 3. Wood anatomy

Deleted: earlywood and latewood diffuse-porous features of the

Deleted: (Fig. 2B) and radiocarbon measurements (Fig. 2C) in selected years before and after the radiocarbon bomb-peak confirmed that

Formatted: Line spacing: single

Deleted: growth periodicity is annual.

Formatted: Font: Bold, Font color: Black

Formatted: Font: Bold, Font color: Black

Deleted: 3B

Deleted: 3-4

Deleted: chronology. Nevertheless, the individual trees

Deleted: common

Deleted: *r*

Deleted: 46

Deleted: = 28

Deleted: that *P. pepei* RW maintained a

Deleted: especially

Deleted: 1909

Deleted: (

Deleted: samples 92

Deleted:) with 22 samples needed to reach such a threshold (SSS > 0.85; Wigley et al. 1984). These

Deleted: (DBH)

Deleted: 33 cm) with an average radial growth of 0.9 mm yr^{-1} .

Years with extremely large RW (95th percentile) included the 1951/52 and 1965/66 growth years (Fig. 2D) which occur before and after a visible growth suppression during the mid-to late 1950s (Fig.2 A, C). Tree rings that began forming in 1906 or 1945 had extremely low values of RW indicating unfavorable growing conditions during the growth-year.

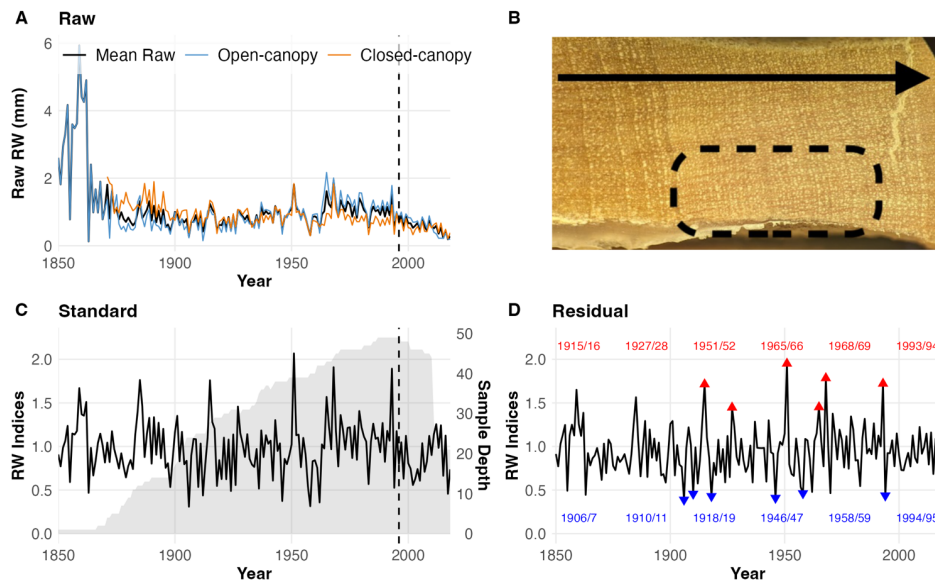


Figure 2. The (A) Raw (C) Standard and (D) Residual RW chronologies of *P. pepei* in Keara. The chronologies (1850-2018) are plotted using the Schulman convention (i.e., anchored on the year of initial ring formation; see section 2.3). (A) There has been a distinct decline in raw (radial) RW since the 1996/1997 growth-year (change point is indicated by the black-dotted line). (A) This decline ($p=0.01$) was evident in both the open-canopy (blue line) and closed-canopy (orange line) forests that were sampled. (B) An image depicts a core sample where several rings are suppressed within a 4 mm distance (dashed circle). The black arrow indicates the direction of radial growth for this core (from left to right). (C) The standard RW is plotted with the mean sample depth of the full network through time (grey shading). Triangles on the residual timeseries (D) signify the years within the top 5th (six smallest growth rings; Blue color) and 95th (i.e. largest growth rings; red color) percentiles of RW since 1900 (SSS > 0.85). Since the tree rings are estimated to form during the wet season (two-calendar years ~October-April), both years are labeled in the colored text (ordered chronologically).

3.2 Monthly climate-growth relationships

The sensitivity of *P. pepei* RW to local climate between 1960-2015 is illustrated by bootstrapped correlations between monthly Pre, Tavg, Tmin, and Tmax in Fig. 3. *P. pepei* RW (standard chronology) positively correlates with Pre variability during the

- Deleted: Notable growth years since 1909 are denoted as ... [51]
- Formatted ... [52]
- Deleted: 3: ... [53]
- Formatted ... [54]
- Deleted: (A), ... [55]
- Formatted ... [56]
- Deleted: (B), ... [57]
- Formatted ... [58]
- Deleted: (C) ... [59]
- Formatted ... [60]
- Deleted: compiled using ... [61]
- Formatted ... [62]
- Deleted: trees from ... [63]
- Formatted ... [64]
- Deleted: (A) ... [65]
- Formatted ... [66]
- Deleted: data shows a decreasing ... [67]
- Formatted ... [68]
- Deleted: trend ... [69]
- Formatted ... [70]
- Deleted: 97 (... [71]
- Formatted ... [72]
- Deleted:). ... [73]
- Deleted: tight growth observed in ... [74]
- Formatted ... [75]
- Deleted: image ... [76]
- Formatted ... [77]
- Deleted: residual chronology ... [78]
- Deleted: changing ... [79]
- Deleted: size (shaded color) for ... [80]
- Deleted: site ... [81]
- Deleted: D ... [82]
- Formatted ... [83]
- Formatted ... [84]
- Formatted ... [85]
- Formatted ... [86]
- Formatted ... [87]
- Deleted: denote ... [88]
- Formatted ... [89]
- Deleted: between 1909-2018. ... [90]
- Formatted ... [91]
- Deleted: 1 ... [92]
- Deleted: Monthly correlation analysis ... [93]

wet season (Fig.3A). There are significant correlations between RW and prior (lag=1) December-March precipitation ($r=0.37$ for January). Correlations with prior-year December ($r=0.20$) weakened when controlling for Tav_g, but current-year November Pre remains robust ($r_p=0.27$). Fig. A4A shows December-March (DJFM) precipitation significantly decreased over the 1960-2015 period at a rate of ~6 mm per decade at the same time there was an observed decline in *P. pepei* RW (Fig. 2A). RW is negatively correlated to prior-year Tav_g DJFM ($r=-0.21$ in March to $r=-0.34$ in February, $p<0.05$). However, after controlling for precipitation effects, partial correlations for Tav_g revealed a positive, robust relationship ($p<0.05$) with RW current-year February to April (FMA) months ($r_p=0.25$ in February to 0.37 in April). *P. pepei* RW also correlates positively with FMA Tmax (Fig. 2D), emphasizing the importance of late-wet season temperature variability near our site on current-year RW as well. Although there were no significant trends in FMA Tav_g between 1960-2015 (Fig. A4 B), there was a significant decrease of Tmax FMA of nearly 0.1°C per decade (Fig. A4 D, $p=0.05$).

Unlike Tav_g, partial correlations indicate RW correlations with prior-year Tmin (Fig. 3C) are significant independent of precipitation variability (i.e. the negative signal persists even when the covariance with precipitation is removed). Negative, significant correlations were found between *P. pepei* RW and prior November- March Tmin (NDJF; $r=-0.28$ in November to $r=-0.35$ in February). It is interesting to note an extreme cold period near Keara during the late 1950s (Tmin, Fig. A5 BC) corresponds with a growth suppression observed in *P. pepei* RW in Fig. 2A and C. Unlike the decrease observed in Tmax near Keara (FMA), NDJF Tmin significantly increased at a rate of 0.1°C per decade ($p=0.02$). In summary *Polylepis pepei* RW is limited by FMA Tmax (positive, current-year relationship) and NDJF Tmin (negative, lagged relationship) for distinct seasons.

Overall *Polylepis pepei* RW is larger under wetter and cooler conditions. However, climate trends since 1960 (Fig. A4) indicate this treeline is facing a warmer and drier November-March (Pre, Tmin) and a cooler wet-to-dry 'shoulder season' months between February- April (Tmax). As mentioned in Section 2.1, Tav_g and Pre are negatively correlated during the wet season (~October-April, $r=-0.27$) in Keara and thus the robust negative correlations between RW temperature (Tmin, Tmax) emphasize the indirect effect of temperature on water availability and thus *P. pepei* tree-growth at treeline. Seasonal averages of DJFM precipitation, NDJF Tmin and FMA Tmax were selected for spatial correlation analyses for the greater tropical south American region.

Moved (insertion) [19]

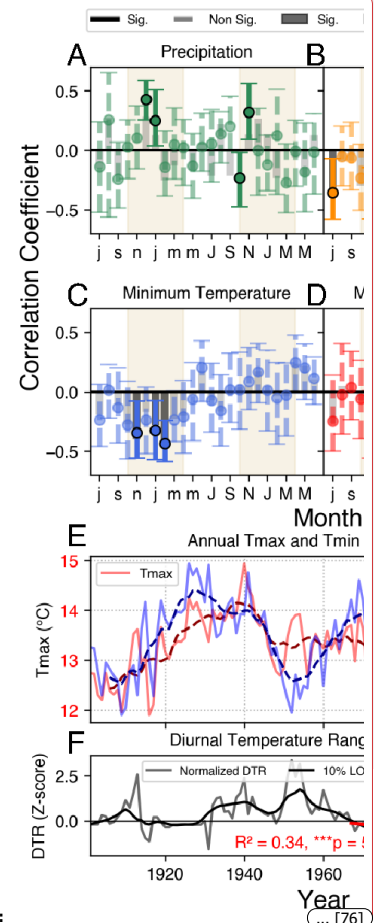
Deleted: the period from July 1981 to June 2018 shows negative correlations with ...recipitation effects, partial correlations for Tav_g revealed a positive, robust relationship ($p<0.05$) with RW current-year February to April (FMA) months ($r_p=0.25$ in February to 0.37 in April). *P. pepei* RW also correlates positively with FMA Tmax (Fig. 2D), emphasizing the importance of late-wet season temperature and positive correlations with precipitation during growing seasons. *P. pepei* RW shows significant positive ... [73]

Deleted: the relationship between temperature and RW was more...W correlations with prior-year Tmin (Fig. 3C) are significant independent of precipitation variability (i.e. the negative mean and minimum temperature ...ignal persists even when the covariance precipitation is removed).
 A robust, negative, temperature relationship with tree growth ... [74]

Formatted: Indent: First line: 0"

Moved up [19]: Fig.

Deleted: 4E). Further, the diurnal temperature range (i.e. difference between maximum and minimum temperature) depicts a Negative, significant negative trend in this region since 1967 which means the rate of increase for minimum temperatures has surpassed that of maximum temperature (Fig. 4F)...orrelations were found between *P. pepei* RW and prior November- March Tmin (NDJF; $r=-0.28$ in November to $r=-0.35$ in February). It is interesting to note an extreme cold period observed in annu... [75]



Deleted: ... [76]

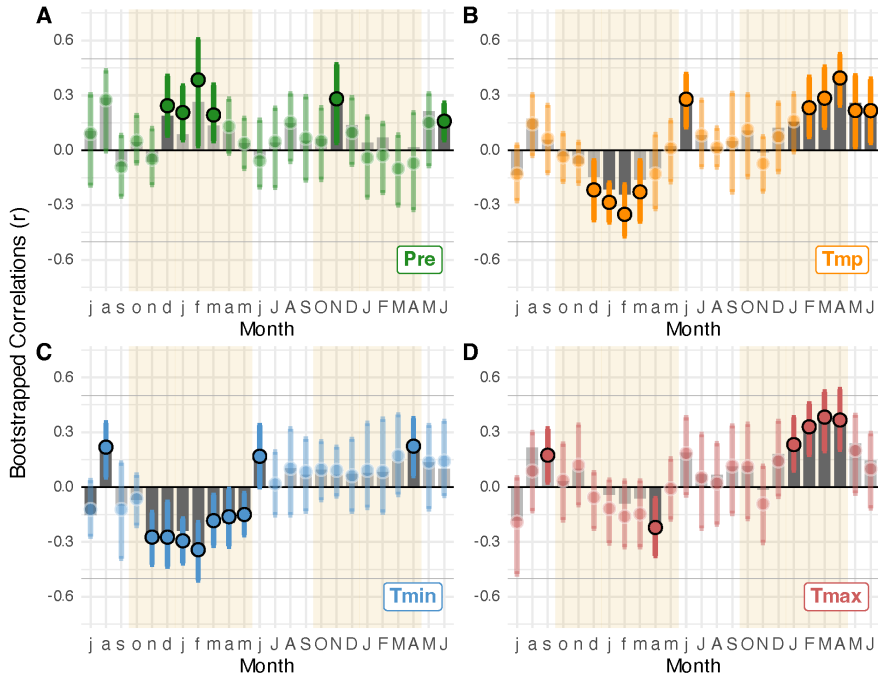


Figure 3: Bootstrapped correlations between *P. pepei* RW and monthly climate from 1960-2015. The x-axis represents months beginning in July of the prior-year (lag=1, lowercase letters) and extending to June of the current year (lag=0, uppercase letters). Tan shading indicates the extended wet period (October- April) for this region of the MNP. **A: green color, precipitation from local station data. B-D: correlations with CRU temperature grid points Tavg(orange), Tmin (Blue), Tmax(red). The median Pearson correlation (r) is represented by colored circles plotted with upper and lower limits of confidence intervals. Partial correlations (r_p) are represented by grey bars. Solid circles and bars indicate significant correlations which are inferred from 95% confidence intervals from the random bootstrapping.**

3.3. *Polylepis pepei* RW, and tropical South American climate variability

Spatial correlations reveal the broader, regional extent of the climate signal recorded in the *P. pepei* RW at the Keara treeline. (Fig. 4). Binomial field tests indicated the spatial extent of significant correlations (black dots; $p < 0.05$) exceeded what would be expected by chance ($p < 0.001$ for all variables). *P. pepei* RW is positively correlated to prior-year DJFM precipitation (CHIRPS; 1981-2015) in most of tropical South America (Fig. 4A). The strongest precipitation signal is observed along the eastern flanks of the Peruvian Andes and the northern Amazon Basin in Brazil. RW is also positively correlated to FMA Tmax in the northern and southern portions of the tropical Andes-Amazon with the strongest values ($r > 0.50$) centralized locally

Deleted: CRU (B-D) for grid points closest to the sites.

Formatted: Font: 10 pt

Formatted: Font: 10 pt

Deleted: t-

Deleted: t

Formatted: Font: 10 pt

Formatted: Font: 10 pt

Deleted: (

Deleted: . Significant correlations are represented by solid lines.

Formatted: Font: 10 pt

Deleted: gray bars show partial correlations with a given variable. (E) Annual minimum (blue line) and maximum (red line) temperatures between 1901-2019 for the nearest CRU gridpoint. (F) The normalized diurnal temperature range, calculated as the difference between Tmax and Tmin, is plotted with a 10-yr smoothing spline and linear trend line since 1967. The R^2 -value and significance of the 1967-2019 trend are included as red text.

Formatted: Font: 10 pt

Formatted: Font: 10 pt

Deleted: Seasonal and spatial climate sensitivity in *P.*

Deleted: ¶

The prior-year climate signal in *P. pepei* RW at treeline is even more robust when compared to seasonal-averages of

Deleted: averaged for 2-months or more between 1981-2019 (Fig. 5). Correlations for 2-6 month averages reveal significant relationships ($p < 0.05$) between RW and precipitation (Fig. 5A) or temperature (Fig. 5B).

Moved down [20]: 5B).

Deleted: The standard RW chronology correlates the strongest with the 3 and 4-month averages of climate, particularly for prior-year OND and NDJ for both temperature and precipitation. Correlations include a positive relationship to precipitation with OND $r = 0.41$ and NDJ $r = 0.40$ and temperature OND $r = -0.45$; NDJ $r = -0.47$ respectively. Because the highest correlation with climate included the negative NDJ relationship to temperature, this ... [77]

Deleted: record between 1981 and 2019

Deleted: 5C, D). Regarding precipitation,

Deleted: seasonal

Formatted: Font: Not Bold

Deleted: 5C

Deleted: (indicated by black dots)

Deleted: locally, extending to

Deleted: central

Deleted: Bolivia and drier regions

Deleted: Southern

near the Bolivian Altiplano. Spatial correlations between *P. pepeii* RW and prior-year NDJF Tmin (CRU 1960-2015) showed significant and negative correlations across most of tropical South America (Fig. 4C), especially near southeastern portions of Brazil. The RW-precipitation correlations also reflect the heterogeneity of precipitation data in mountain areas, whereas the temperature fields are more uniform.

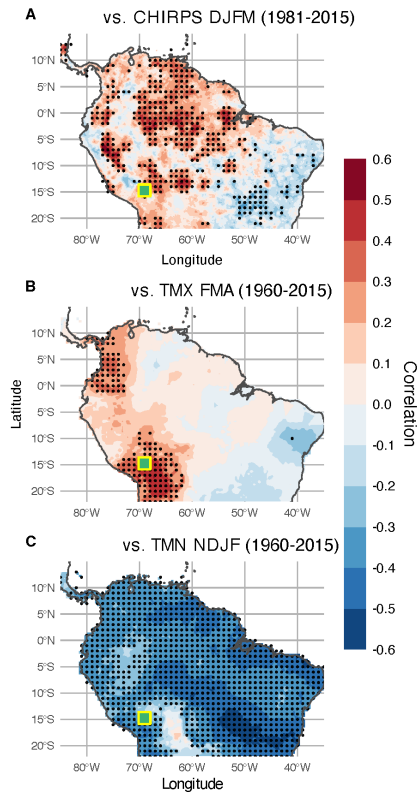
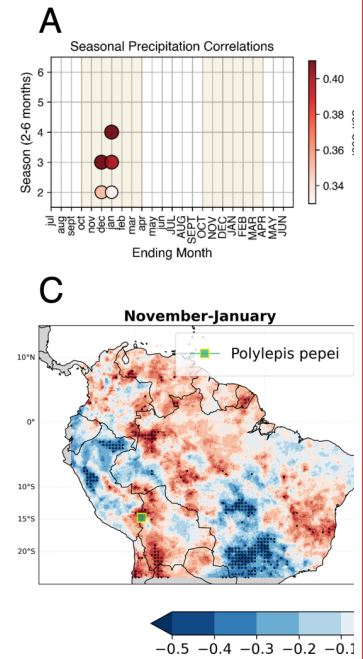


Figure 4. Spatial correlations between *P. pepeii* RW and (A) CHIRPS DJFM precipitation (1981-2015, lag=1), (B) CRU NDJF Tmin (1960-2015, lag=1), and (C) CRU FMA Tmax (1960-2015, lag=0). Black dots represent the areas where there are significant correlations ($p < 0.05$). Binomial field tests indicated there were more significant cells than expected by chance ($p = 0.05$) for all variables (field test $p < 0.001$).

Deleted: patterns of correlation ...correlations between *P. pepeii* RW and gridded temperatures show...rior-year NDJF Tmin (CRU 1960-2015) showed significant and negative ($r > -0.50$) ...o... [78]

Formatted: Font color: Auto



Deleted:

Cor
... [79]

Deleted: RW- NDJ

Formatted: Font: 10 pt

Formatted:

... [80]

Formatted: Line spacing: single

Deleted: and temperature (D) for the period 1981-2019.

Formatted:

... [81]

Deleted:

Deleted: RW is lagged $t-1$ to account for the seasonality of the prior-year growing season. The NDJ season was selected based on moving bootstrapped seasonal correlations with grid... [82]

Deleted: increase in minimum temperature range was reported between the 2021-22 wet season as well as the three other wet seasons ($p < 0.0001$), while non-significant differences were... [83]

Formatted: Font: 10 pt

Formatted: Font: Bold, Font color: Black

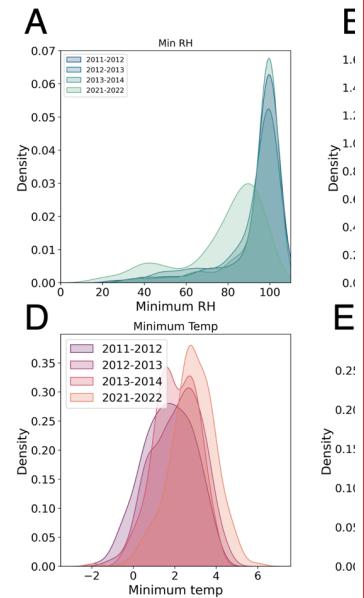
Deleted: three seasons had higher values than of (min, max, mean) RH than in 2021-22. Conversely, the range of minimum and... [84]

Formatted: Font: Bold, Font color: Black

Formatted: Font: Bold, Font color: Black

3.4 Growth response of treeline *P. pepei* to extreme climate events

The impact of extreme DJF-ENSO events on climate and the residual RW chronology is shown in Figure 5. Table A1 lists the years of known moisture anomalies in tropical South America connected to El Niño (warmer SST) or La Niña (cooler SST) conditions in the Pacific Ocean. Regardless of the time span and spatial resolution, climate datasets show El Niño DJF events were linked to drier and warmer conditions while extreme La Niña DJF years were wetter and cooler (Fig. 5AB). SEA results for El Niño-DJF years show there was a one-year delayed and negative RW response, i.e., one year after an event, *P. pepei* showed a decrease in radial growth ($\alpha = 0.1$). Although there was a non-significant growth increase in RW after a La Niña-DJF, there was a significant negative response three years after an extreme DJF-La Niña (Fig. 5B). It's interesting to note however, the largest growth ring observed in *P. pepei* formed during the 1950-1951 wet season and correspond to extreme La Niña events in DJF 1950 and 1951 (Fig. 2C). The smallest (5th percentile) growth ring in 1906-07 occurred after a major DJF-El Niño event in 1905. In summary, *P. pepei* RW at the Andes-Amazon treeline has a lagged significant response to extreme DJF-ENSO conditions.



Deleted:

[85]

Deleted: 5

Deleted: (Table 1) ... climate and the residual RW (Fig. 3B) were conducted using SEA methods (Fig. 7A, B). Normalized growth... chronology is shown in Figure 5. Table A1 lists the years of known moisture anomalies (Z-scores) are shown for the four years before and after the event ($t=0$) to assess the timing and significance of the RW anomaly. The impact of drought during ... tropical America connected to El Niño years shows a lagged ($t+1$) at ... [86]

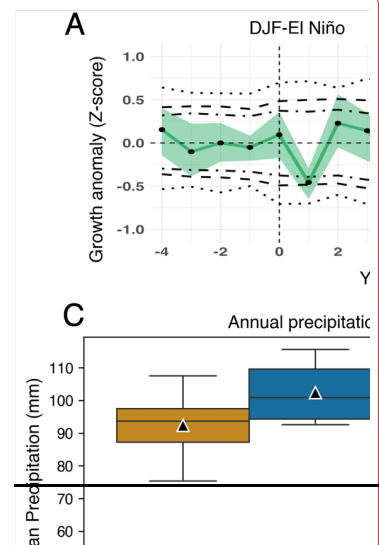
Deleted: both precipitation... climate datasets show that the 24 ... Niño extremes during the peak wet-season (...DJF) are... events were linked to drier and warmer conditions in the study region, and DJF... hile extreme La Niña events... DJF years were associated with ... etter annual precipitation overall. CRU temperature data showed El Niño conditions were also warmer (Figure 7D). (... [87]

Formatted: Font: Italic

Formatted: Font: Italic

Moved (insertion) [20]

16



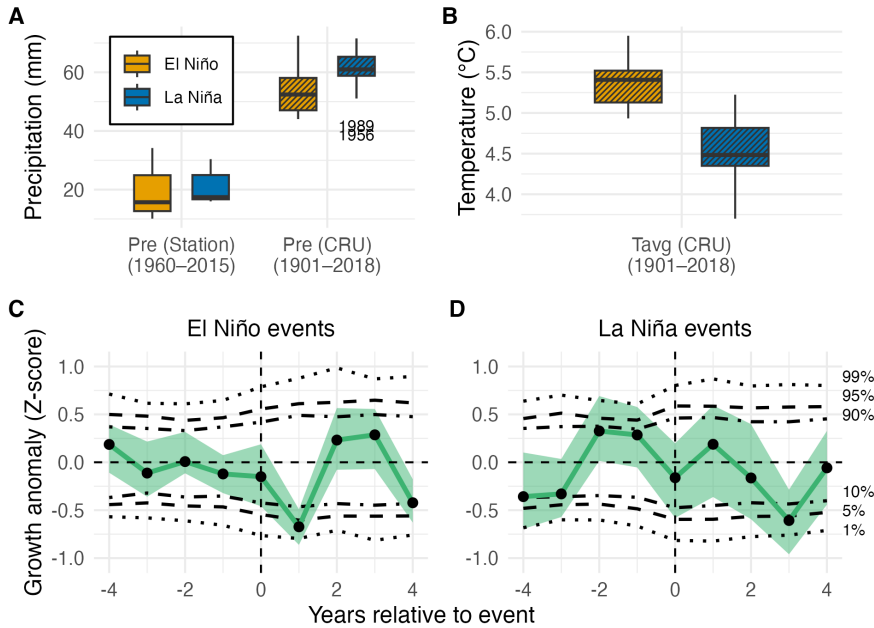


Figure 5: Boxplots showing annual (A) precipitation and (B) temperature for the 26 years of extreme DJF-ENSO events, using both station and CRU data. Outlier years in the CRU precipitation data are labeled in (A). Annual mean climate during El Niño-DJF is represented as orange colors, while La Niña is shown in blue ($n = 13$ years per event). Superposed epoch analysis of the residual RW response between 4 years before and 4 years after ENSO events (C, D). The uncertainty of the growth response is depicted as green shading. Horizontal black lines represent confidence intervals (two-tailed significance thresholds: 10-90%, 5-95% 1-99%) based on stationary bootstrapping.

Deleted: ($t = -4$), during ($t = 0$),

Deleted: ($t = -4$) years of known to the top 12 DJF-El Niño (A) and DJF- La Niña

Deleted: B). Dashed

Deleted: double

Deleted: while the uncertainty of the response is depicted as green shading. (C) Annual precipitation boxplots using the CHIRPS (left) and CRU gridpoints for the (top 24) years of extreme DJF-ENSO, using the nearest. El Niño-related events are represented in orange colors, while La Niña is shown blue. (D) Annual temperature during these events using CRU gridpoint data...

4. Discussion

4.1. Radial growth decline and climate sensitivity of a tropical treeline site in Bolivia

Annual RW chronologies of *P. pepei* from a high Andean Amazon forest in Bolivia have been presented and analyzed. This is the first tree-ring record for this species in Madidi National Park and the longest record of *P. pepei* RW chronology in South America (1850-2018). This record provides new information about tree growth and climate sensitivity in an understudied tropical treeline in South America (~3800-4400 m.a.s.l.). The potential human influence on RW for trees in Andes-Amazon forests should be considered when evaluating the growth patterns at tropical treelines in this region. For the *P. pepei* near Keara, the lower elevation open-canopy forest (3795-4100 m.a.s.l.) showed possible fire scars in the 1940s and clear forest fragmentation related to cattle ranching. This subpopulation is likely more threatened by human activities than the closed canopy site between 4000-4400 m.a.s.l. sampled in 2019 (Fig. 1CD). Despite the potential for local environmental effects on growth, correlations between *P. pepei* RW and local climate are robust and may signify a response to regional shifts in hydroclimate patterns observed in tropical South America.

We found that *P. pepei* RW is limited by prior-year temperature and precipitation variability during the wet season, with larger RW in the subsequent growth year when it was wetter and colder (Figs. 3 and 4). This is consistent with previous studies showing *Polylepis* ring-width positively correlated with previous growing-season water availability in the Andes (Argollo et al. 2004, Morales et al. 2004, Christie et al. 2009, Soliz et al. 2009, Crispín-DelaCruz et al. 2022, Rodríguez-Caton, et al. 2021). Although the RW-precipitation correlations were robust, our results suggest that this *P. pepei* treeline is likely more affected by temperature-related moisture-stress changes (Fig. A4), as would be expected particularly at treeline (Fritts, 1976). A pronounced decline in radial growth since 1997 (Fig. 2A) was observed at the same time this region has endured warmer and drier austral summers (~November-March) in recent decades (Figs. A4, A5). The Keara treeline also revealed an imprint of extreme ENSO-related events in *P. pepei* growth rings.

Hot-drought conditions related to DJF-El Niño events had a significant negative impact on radial growth of *P. pepei* at our study site. Although La Niña SEA were inconclusive, the lagged negative effect ($t=-3$) may be related to the occurrence of El Niño events in years after La Niña. DJF anomalies were selected for analyses because it is the mature phase of the summer monsoon (70% of annual rainfall), but the use of annual (instead of seasonal) events may show larger impacts on RW.

Future advances of this treeline towards higher elevations (Fig. 1C) are unlikely due to local geomorphologic constraints (Macias-Fauria and Johnson, 2013) and thermal niches that are required for subalpine recruitment (Kessler et al., 2014; Körner and Hoch, 2023). As mentioned in the Introduction, *Polylepis pepei* in the tropical Andes is adapted to cold soil temperatures (3-5°C). Although the future spatial extent of the *P. pepei* forest under warming is uncertain, our study provides insight into

Deleted: .

Deleted: , seasonally humid

Deleted: northwestern

Deleted: A new annually-dated

Deleted: for the MNP

Deleted: novel and robust

Deleted: at the

Deleted: (4000

Deleted:), in an understudied biodiversity hotspot in South America. There is a decline in mean radial growth that is particularly pronounced since 1997 (Fig 3C). This decline can also be seen visually in some samples from the drier (talus-slope) site in Keara (Fig 1C).

Deleted: of these Andean forests.

Deleted: subset (~3700-4000

Deleted: , north and west of the talus slope site)

Deleted: (Figure 1C). Nevertheless, dendrochronological approaches made it possible to explore the climate signal recorded in the annual rings.

Deleted: variability

Deleted: .

Deleted: network

Deleted: ,

Deleted: elevational

Deleted: Extreme El Niño and La Niña

Deleted: during the peak summer monsoon bring dry/warm and wet/cool conditions may amplify or reduce the effect of precipitation and temperature variability on

Deleted: . Overall

Deleted: 3-year

Deleted: events

Deleted: where the tropical Andes receives

Deleted: ,

Deleted: or NDJ related ENSO

Deleted: trees studied herein

Deleted: (Kessler et al., 2014; Körner and Hoch, 2023) that are requirements for subalpine recruitment. Studies

Moved up [11]: of *P. pepei* sites between 3800-4300 m.a.s.l.

Deleted: in Peru (Kessler et al., 2014) and Bolivia (Hoch and Körner, 2005) recorded soil temperatures (> 5cm) ranging from 3-5°C during the wet season, highlighting the cold-adapted conditions of this species in the eastern tropical Andes. Despite local soil conditions and human activities that impact the shape of Andean treelines like those for *Polylepis* (Bader et al., 2007), the optimal thermal niche for woody plants is the leading abiotic factor that defines the spatial extent of such forests across the globe (H... [89])

the limiting factors to radial growth at a tropical Andean treeline in Bolivia since 1960. In the following sections we discuss potential local environmental and climate variables that may contribute *P. pepei* tree-ring variability in Keara.

4.2. Changes in temperatures and humidity at the *P. pepei* treeline in Bolivia

Increases in minimum temperature (T_{min}) may be reducing moisture availability in high-elevation Andean tropical sites. Hourly climate data recorded by data loggers at our *P. pepei* site (Fig. A3) showed that the period September 2021-May 2022 had significantly warmer T_{min} and lower relative humidity (RH) in comparison to the period 2011-2014 ($p < 0.0001$). This decrease in RH alongside an increase in temperature suggests that the capacity of air to hold moisture has outpaced the actual moisture content, making the air drier despite higher temperatures. Although these results cover a short time-window, they provide *in situ* evidence of warming and drying trends observed in the climate data of this site (Fig. A4). DTR variability (i.e. difference between T_{max} and T_{min}) near Keara in Fig. A5 depicts a significant negative trend in this region since 1960, which means the rate of increase for minimum temperatures has surpassed that of maximum temperature. Even though warmer temperatures increase the capacity of the air to hold more water vapor (i.e., the Clausius-Clapeyron relation), if the moisture supply does not increase proportionally, humidity will decrease.

P. pepei had significant negative correlations with increasing minimum temperatures on the local and spatial scale (Figs. 3 and 4). Minimum temperatures influence convection, as rainfall in the Andes-Amazon ecotone largely occurs in the afternoon/night when radiative cooling drives cold air downslope and converges with rising warm moist air from the tropical lowlands (Garreaud, 1999; Junquas et al., 2018; Romatschke and Houze, 2010). Known as 'orographic precipitation', this process is key for rainfall distribution across elevations in the Andean foothills like our site (Arias et al., 2021; Chavez and Takahashi, 2017). In the region of the MNP, maximum precipitation occurred between 1000-1300 m.a.s.l., with a sharp decrease in moisture distribution towards higher elevations > 3000 m.a.s.l. (Chavez and Takahashi, 2017). If minimum temperatures increase, the radiative cooling effect is weaker, which may result in warm, moist air converging at lower elevations, below our treeline *P. pepei* site (Romatschke and Houze, 2010). The hourly meteorological data between September-May in 2011-14 and 2022-23 shows that RH peaks at 3:00 P.M. in Keara on average, suggesting afternoon cloud formation. It's interesting to note the declining RW trends observed in *P. pepei* (>3800 m.a.s.l.) diverge from the increasing RW trends observed in lower-elevation humid forests from MNP since the 1980s (e.g. *Juglans boliviana* ~1300 m.a.s.l., Oelkers et al., 2023). It is possible that the increase in T_{min} since the late 20th century (Fig. A5) may have contributed to reduced orographic convection and moisture availability, thus potentially limiting the growth of *P. pepei*. Future research needs to be conducted on horizontal moisture transport in the Andes-Amazon and the diverging trends in growth between the lower Amazon and treeline forests.

Besides inhibiting moisture convergence and transport from lower elevations, warmer minimum temperatures could also affect the tree water-balance in Keara by increasing transpiration and respiration rates (Sierra et al., 2022). A global analysis of tropical tree longevity using tree-ring and other data found that tree mortality is increasing in all tropical biomes due to heat-

Deleted: 1981.

Formatted: Font: Bold

Deleted: minimum

Deleted: relative

Deleted: Although the shortness of the high-resolution CHIRPS dataset limits our interpretation of the role of

Deleted: before 1981 on observed growth trends, the long-term CRU temperature datasets show a significant decline in the diurnal temperature range (Fig. 4F), driven by rising minimum temperatures (Fig. 4 E).

In agreement, daily climate

Deleted: in the

Deleted: in the *Polylepis* forests

Deleted: 6) confirmed

Deleted: -May in

Deleted: as having

Deleted: nighttime/early morning conditions (reflected by minimum temperatures

Deleted: 2012

Deleted: Despite the fact that higher temperatures increase the capacity of the air to hold more water vapor (i.e. "Clausius-Clapeyron" relation), if the moisture supply does not increase proportionally the humidity will decrease.

Deleted: is indeed what was observed from the RH data recorded *in situ* that showed significant decreases in minimum, maximum and mean RH at our study forests. In short, a

Deleted: Further, analyses

Deleted: gridded CRU

Deleted: and

Moved (insertion) [21]

Moved (insertion) [22]

Deleted: CHIRPS

Moved (insertion) [23]

Moved (insertion) [16]

Formatted: Strikethrough

1777 related water stress and increased evaporative demand at the leaf level (Locosselli et al., 2020). From an ecophysiological
1778 perspective, respiration rates increase with rising temperatures and without photosynthesis occurring at night. This in turn
1779 increases the amount of carbon (and water) released from the trees to the atmosphere. Temperature and precipitation near the
1780 *P. pepei* site are inversely correlated during the extended wet season (October-April, $p < 0.05$). If there is less cloud cover (and
1781 rainfall), there is higher solar irradiance and temperatures, which may limit the photosynthetic capacity of tropical trees at
1782 higher elevations (García-Núñez et al., 2004; Hoch and Körner, 2005; Jaramillo, 2015). The current-year positive relationship
1783 between RW and FMA Tmax (Fig.3C, Fig. 4.B), may also highlight the ecophysiological link between tree-ring size (i.e.
1784 xylogenesis) and cooler trends in Tmax at the end of the wet season between 1960-2015 (see discussion in Rodriguez-Caton
1785 et al. 2021). Although it is possible that the timing of the mechanisms controlling primary (photosynthesis) and secondary
1786 growth (wood formation) may not occur at the same time, the RW-climate correlations show there is less radial growth if is
1787 warmer and drier than when it is cooler and wetter (Figs. 3, A4). Further research must be conducted to determine the
1788 phenology and physiological response of *P. pepei* to micro-climate conditions such as a reduction in orographic precipitation
1789 at treeline or low soil-water availability.

1791 4.3. Large-scale climate variability impacting tree growth in tropical Andean treelines

1792 The recent decline in radial growth may be also influenced by broader scale hydroclimate changes. In the central Andes
1793 treeline, ($>17^{\circ}\text{S}$; 4657-4800 m.a.s.l.). Negative RW trends in *P. tarapacana* were attributed to increasing drought conditions
1794 in southern Peru and northern Chile since the 1970s. Morales et al. (2023) developed a NDJ precipitation reconstruction from
1795 these trees and discovered that a drying trend since 1997 was unprecedented in the 389-yr reconstruction. Although 1997 was
1796 identified as a changepoint in the raw ring-width data of *P. pepei*, our site is in the Amazon basin, a much more humid
1797 environment than the *P. tarapacana* in Morales et al. (2023). Nonetheless the shared timing of growth decline in these high-
1798 Andes forests is interesting.

1800 Increasing drought frequency in the tropical Andes and southern Amazon Basin ($> \sim 15^{\circ}\text{S}$) has been linked to delayed wet
1801 season onset (Espinoza et al., 2016; Fu et al., 2013; Marengo et al., 2011). One possible explanation is an intensification of the
1802 atmospheric Hadley circulation, related to warming in the (northern) tropical Atlantic Ocean, which interrupts upward flows
1803 from the Amazon to the Andes during the dry-to-wet period (Beveridge et al., 2024; Espinoza et al., 2021, 2019; Yoon and
1804 Zeng, 2010). In particular, Ronchail et al. (2018) and Espinoza et al. (2019) found a significant increase in dry-day frequency
1805 between September-November in Bolivia and Peru which marks a delay in the timing of austral spring rainfall. Additionally,
1806 an observed weakening of upper-level easterlies winds from the Amazon to the Andes (Segura et al. 2022), may have
1807 contributed to reduced moisture transport potentially affecting tropical treelines like *P. pepei* in Keara.

1809 In contrast to a drier start to the wet-season, a recent increase in precipitation at the end of the wet season < 2000 m.a.s.l. has
1810 been observed in lowland regions of the northern Amazon and Andes-Amazon (Arias et al., 2021; Espinoza et al., 2021, 2019;

Moved (insertion) [5]

Deleted: data near the *P. pepei* site. From an ecophysiological perspective, respiration rates increase with rising temperatures and without photosynthesis occurring at night. This in turn increases the amount of carbon (and water) released from the trees to the atmosphere. Temperature and precipitation near the *P. pepei* site are inversely correlated during the extended wet season (October-April). For example, if $p < 0.05$. If there is less cloud cover (and less precipitation)... rainfall, there is higher solar irradiance and temperatures, which may limit the photosynthetic capacity of these... tropical trees at higher elevations (García-Núñez et al., 2004; Hoch and Körner, 2005; Jaramillo, 2015). The current-year positive relationship between RW and FMA Tmax (Fig.3C, Fig. 4.B), may also highlight the ecophysiological link between tree-ring size (... [90])

Moved up [21]: radiative cooling drives cold air downslope and converges with rising warm moist air from the tropical lowlands

Moved up [22]: (Arias et al., 2021; Chavez and Takahashi, 2017).

Moved up [23]: (Chavez and Takahashi, 2017).

Moved up [14]: have deteriorated forest structure and health, with increasing loss of forest cover in recent years (Finer and

Moved up [15]: 2014). These losses of primary forests have severe implications for carbon storage capacity, ecosystem function,

Deleted: Minimum temperatures influence convection, as rainfall in the Andes-Amazon ecotone largely occurs in the afternoon (... [91])

Deleted: Known as 'orographic precipitation', this process is key for rainfall distribution across elevations in the Andean foot (... [92])

Deleted: A study on southern Peruvian rainfall hotspots (which included our study area in MNP) used radar-based precipitation (... [93])

Deleted: However, if minimum temperatures are warmer, the radiative cooling effect is weaker, which means that warm, (... [94])

Deleted: local soil-water balance by increasing transpiration, respiration rates and overall water loss in this forest (Sierra (... [95])

Deleted: *pepei* studied herein, is at great risk of endangerment due to habitat loss related to fires and land conversion for cattle (... [96])

Deleted: (... [97])

Formatted: Strikethrough

Deleted: observed at our *P. pepei* site ... in MNP (14°S) near the southwestern Amazon Basin aside from factors described at (... [98])

Moved up [12]: Southwest of our *P. pepei* site, in the central Andes of southern Peru ice proxy data indicated recent surface

Moved up [13]: Hoffmann and Weggenmann, 2013).

Deleted: In November 2009 near Keara, temperatures were so warm that a catastrophic glacial lake outburst flood eliminated (... [99])

Deleted: (... [100])

Deleted:), especially since the 1990s ... has been linked to delayed wet season onset (Espinoza et al., 2016; Fu et al., (... [101])

Moved (insertion) [25]

2236 Malhi et al., 2008; Zanin and Satyamurty, 2020). These studies argue that warming of the Atlantic Ocean, land-surface changes
2237 in the Amazon, and wind anomalies are the primary factors contributing to changes in specific humidity in tropical south
2238 America overall (particularly between March-May; see references in (Beveridge et al., 2024)). Within Bolivia, contrasting
2239 trends in precipitation and tree-growth have been observed between low and highland elevation forests. Tree-ring oxygen
2240 isotopes ($\delta^{18}\text{O}$ from *C. odorata* in the lowland Bolivian Amazon (10°5'S, 66°18'W; 106 m.a.s.l.) reflected an increase in
2241 November-March precipitation (and decrease in $\delta^{18}\text{O}$) between 1980-2010 (Baker et al., 2016; Cintra et al., 2025), while
2242 treeline *P. tarapacana* in the Bolivian Altiplano (22.3°S, 67.23°W; ~4600 m.a.s.l.) recorded a pronounced dry period for
2243 December-March precipitation between 1992-2012 (Rodriguez-Caton et al., 2024). Despite the fact that these hydroclimate
2244 trends are complex and spatially variable, having *in situ* high-resolution climate proxies at the Andes-Amazon treeline such as
2245 *P. pepei* may be useful in understanding long-term changes in orography.

2246
2247 Overall, growth variability at this *P. pepei* treeline in the Andes-Amazon here may be related to temperature-driven moisture
2248 trends observed at local and regional scales. This study herein has demonstrated the dendroclimatic potential of this species at
2249 a treeline from the most biodiverse region of the world (MNP; Muller, 2017) and provided insight into the growth response of
2250 a tropical forest in South America under a warming environment.

2251 5. Conclusions

2252 We reported a significant decline in radial growth in a tropical *P. pepei* treeline in Kearsa, Bolivia, at the edges of the Andes-
2253 Amazon high-elevation forests. Here, growth decreases with warmer and drier conditions in the prior-year wet season, and there
2254 is an adverse influence of temperatures, in particular T_{min} , on growth. Higher T_{min} weakens the nighttime convection that
2255 brings moisture from lower elevations to this site, and in general, warmer conditions increase evaporative demands and cause
2256 water stresses. We also found a tendency of narrower growth rings in the year following El Niño events, while the role of La
2257 Niña events was inconclusive. This asymmetric influence of ENSO on tree growth warrants further investigations. Moving
2258 forward, since we found *P. pepei* to develop annual rings that are climate sensitive, expanding the *P. pepei* network in Kearsa
2259 would enable reconstructions of precipitation and temperature of the southwestern Amazon-Andes ecotone. This would be the
2260 first of its kind for northern Bolivia, extending the limited station records to the mid-1800s. Our results provide new insights
2261 into the response of a tropical treeline in an era of global warming, increasing climate extremes, and human activities, and
2262 support future dendrochronological research of *P. pepei* in South America. We recommend pursuing research that focus on
2263 quantifying leaf respiration and temperature response to better understand the ecophysiology of this tropical treeline species
2264 in Bolivia.

Deleted: Overall, the recent negative trend of *P. pepei* RW studied here may be related to temperature-driven moisture trends observed on both

Deleted: to climatic change. High mountain paleoclimate proxies, like our *P. pepei* site, independently show how temperature-driven humidity changes modify natural environments in tropical South America

Deleted: ¶

Formatted: Font: 10 pt

Deleted: composed by *P. pepei*, in contrast to growth increases that have been observed in mid-

Moved up [25]: (Arias et al., 2021; Espinoza et al., 2021, 2019; Malhi et al., 2008; Zanin and Satyamurty, 2020).

Deleted: species from the same area of MNP (e.g. *Juglans boliviana*, Oelkers et al. 2023). Several studies have reported on the observed increased dry season length in the southern Amazon and central tropical Andes, while lowland areas such as the northern Amazon and Andes-Amazon basin (< 2000 m.a.s.l.) are becoming wetter in the wet-dry season

Deleted: Our results show that the observed decline in *P. pepei* treeline may be associated with increases in minimum temperatures driven a reduction of available moisture through different mechanisms resulting in drought stress. Climate-growth correlations showed *P. pepei* RW was smaller if the

Deleted: was warmer and drier at the Kearsa treeline: By

Formatted: Font color: Custom Color(RGB(34,34,34))

Deleted: and the tropical Andes, there is the potential for

Deleted: , and thus drought, for

Deleted: Central

Deleted: (~30 years in length on average) back to at least the

Deleted: The

Deleted: presented herein have provided

Deleted: Andean

Deleted: the use of dendrochronology in

Deleted: tropical forests.

Deleted: ¶

2300 **Author contribution**

2301 Co-authors LAH, DRC, MRC, MEF, RO, ET, AF collected tree samples in Keara. CM and AF organized field campaigns and
2302 provided essential information regarding Madid National Park. RDD and LAH assisted in initial experimental design and
2303 editing. Tree-ring dating, measuring, and analyses was conducted by corresponding other RO. HTTP, aided in correlation
2304 analyses and concept. APS assisted in wood anatomical methods. Editorial review provided by all co-authors. Site images for
2305 Fig. 1 were taken by RO.

2306 **Competing interests**

2307 The authors declare that they have no conflict of interest

2308 **Acknowledgements**

2309 This work was made possible by the following funding sources from the U.S. National Science Foundation: AGS-1702789,
2310 AGS-1903687, AGS-2303524, and OISE-1743738. We acknowledge the NSF AGS-1903690 grant at UC Irvine KCCAMS
2311 facility for seven radiocarbon measurements. E.T. received funding from the Comunidad de Madrid program Atracción
2312 Talento “César Nombela” grant number 2023-T1/ECO-29118. This work is dedicated to Renaud, his family and the
2313 community of Keara for their hospitality, knowledge, and assistance in the field. Special thanks to the Nacional Herbario in La
2314 Paz, including Alfredo Fuentes and Freddy “Zen” Ruiz, for their guidance during the 2012 and 2019, 2023 Bolivian field
2315 campaigns.

Deleted: We would also like to thank

Deleted: to Freddy “Zen” Ruiz from

Deleted: his

2316 **Data Availability**

2317 The Polylepis pepel RW chronology from Keara will be made publicly available on the NOAA International Tree-ring
2318 Database.

Deleted: 1

Deleted: final

2B25

2B26

2B27

2328

References

- 2B29 [Argollo, J., Soliz, C., Villalba, R., 2004. Potencialidad dendrocronológica de *Polylepis tarapacana* en los Andes Centrales de](#)
 2B30 [Bolivia. *Ecol. En Bolív.* 39, 5–24.](#)
- 2B31 [Büntgen, U., Wacker, L., Galván, J.D., Arnold, S., Arseneault, D., Baillie, M., Beer, J., Bernabei, M., Bleicher, N., Boswijk,](#)
 2B32 [G., Bräuning, A., Carrer, M., Ljungqvist, F.C., Cherubini, P., Christl, M., Christie, D.A., Clark, P.W., Cook, E.R.,](#)
 2B33 [D'Arrigo, R., Davi, N., Eggertsson, Ó., Esper, J., Fowler, A.M., Gedalof, Z., Gennaretti, F., Griebinger, J., Grissino-](#)
 2B34 [Mayer, H., Grudd, H., Gunnarson, B.E., Hantemirov, R., Herzig, F., Hessler, A., Heussner, K.-U., Jull, A.J.T.,](#)
 2B35 [Kukarskih, V., Kiryanov, A., Kolář, T., Krusic, P.J., Kyncl, T., Lara, A., LeQuesne, C., Linderholm, H.W., Loader,](#)
 2B36 [N.J., Luckman, B., Miyake, F., Myglan, V.S., Nicolussi, K., Oppenheimer, C., Palmer, J., Panyushkina, I., Pederson,](#)
 2B37 [N., Rybníček, M., Schweingruber, F.H., Seim, A., Sigl, M., Churakova \(Sidorova\), O., Speer, J.H., Synal, H.-A.,](#)
 2B38 [Tegel, W., Treydte, K., Villalba, R., Wiles, G., Wilson, R., Winship, L.J., Wunder, J., Yang, B., Young, G.H.F., 2018.](#)
 2B39 [Tree rings reveal globally coherent signature of cosmogenic radiocarbon events in 774 and 993 CE. *Nat. Commun.*](#)
 2B40 [9, 3605. <https://doi.org/10.1038/s41467-018-06036-0>](#)
- 2B41 [Crispín-DelaCruz, D.B., Morales, Mariano.S., Andreu-Hayles, Laia., Christie, Duncan.A., Guerra, A., Requena-Rojas,](#)
 2B42 [Edilson.J., 2022. High ENSO sensitivity in tree rings from a northern population of *Polylepis tarapacana* in the](#)
 2B43 [Peruvian Andes. *Dendrochronologia* 71, 125902. <https://doi.org/10.1016/j.dendro.2021.125902>](#)
- 2B44 [D'Arrigo, R., Jacoby, G., Free, M., Robock, A., 1999. Northern Hemisphere Temperature Variability for the Past Three](#)
 2B45 [Centuries: Tree-Ring and Model Estimates. *Clim. Change* 42, 663–675. <https://doi.org/10.1023/A:1005471918574>](#)
- 2B46 [Farfan-Rios, W., Feeley, K.J., Myers, J.A., Tello, S., Sallo-Bravo, J., Malhi, Y., Phillips, O.L., Baker, T.R., Nina-Quispe, A.,](#)
 2B47 [García-Cabrera, K., 2025. Amazonian and Andean tree communities are not tracking current climate warming. *Proc.*](#)
 2B48 [Natl. Acad. Sci. 122, e2425619122.](#)
- 2B49 [MacDonald, G. m. Kremenetski, K. v. Beilman, D. w, 2007. Climate change and the northern Russian treeline zone. *Philos.*](#)
 2B50 [Trans. R. Soc. B Biol. Sci. 363, 2283–2299. <https://doi.org/10.1098/rstb.2007.2200>](#)
- 2B51 [Politis, D.N., Romano, J.P., 1994. The Stationary Bootstrap. *J. Am. Stat. Assoc.* 89, 1303–1313.](#)
 2B52 [<https://doi.org/10.1080/01621459.1994.10476870>](#)
- 2B53 [Rodríguez-Caton, M., Andreu-Hayles, L., Daux, V., Vuille, M., Varuolo-Clarke, A.M., Oelkers, R., Christie, D.A., D'Arrigo,](#)
 2B54 [R., Morales, M.S., Palat Rao, M., Srur, A.M., Vimeux, F., Villalba, R., 2022. Hydroclimate and ENSO Variability](#)
 2B55 [Recorded by Oxygen Isotopes From Tree Rings in the South American Altiplano. *Geophys. Res. Lett.* 49,](#)
 2B56 [<https://doi.org/10.1029/2021GL095883>](#)
- 2B57 [Rodríguez-Caton, M., Andreu-Hayles, L., Morales, M.S., Daux, V., Christie, D.A., Coopman, R.E., Alvarez, C., Rao, M.P.,](#)
 2B58 [Aliste, D., Flores, F., Villalba, R., 2021. Different climate sensitivity for radial growth, but uniform for tree-ring](#)
 2B59 [stable isotopes along an aridity gradient in *Polylepis tarapacana*, the world's highest elevation tree species. *Tree*](#)
 2B60 [Physiol. 41, 1353–1371. <https://doi.org/10.1093/treephys/tpab021>](#)
- 2B61 [Rodríguez-Caton, M., Morales, M.S., Rao, M.P., Nixon, T., Vuille, M., Rivera, J.A., Oelkers, R., Christie, D.A., Varuolo-](#)
 2B62 [Clarke, A.M., Ferrero, M.E., Magney, T., Daux, V., Villalba, R., Andreu-Hayles, L., 2024. A 300-year tree-ring](#)
 2B63 [\$\delta^{18}\text{O}\$ -based precipitation reconstruction for the South American Altiplano highlights decadal hydroclimate](#)
 2B64 [teleconnections. *Commun. Earth Environ.* 5, 1–13. <https://doi.org/10.1038/s43247-024-01385-9>](#)
- 2365 Akaike, H., 1974. A new look at the statistical model identification. *IEEE Trans. Autom. Control* 19, 716–723.

Formatted: Heading 1

2366 Álvarez, C., Veblen, T.T., Christie, D.A., González-Reyes, Á., 2015. Relationships between climate variability and radial
2367 growth of *Nothofagus pumilio* near altitudinal treeline in the Andes of northern Patagonia, Chile. *For. Ecol. Manag.*
2368 342, 112–121. <https://doi.org/10.1016/j.foreco.2015.01.018>

2369 Andreu-Hayles, L., Tejedor, E., D'Arrigo, R., Locosselli, G.M., Rodríguez-Catón, M., Daux, V., Oelkers, R., Pacheco-Solana,
2370 A., Paredes-Villanueva, K., Rodríguez-Morata, C., 2023. Dendrochronological advances in the tropical and
2371 subtropical Americas: Research priorities and future directions. *Dendrochronologia* 81, 126124.
2372 <https://doi.org/10.1016/j.dendro.2023.126124>

2373 Arias, P.A., Garreaud, R., Poveda, G., Espinoza, J.C., Molina-Carpio, J., Masiokas, M., Viale, M., Scaff, L., van Oevelen, P.J.,
2374 2021. Hydroclimate of the Andes Part II: Hydroclimate Variability and Sub-Continental Patterns. *Front. Earth Sci.* 8.
2375 <https://doi.org/10.3389/feart.2020.505467>

2376 Batllori, E., Gutiérrez, E., 2008. Regional tree line dynamics in response to global change in the Pyrenees. *J. Ecol.* 96, 1275–
2377 1288. <https://doi.org/10.1111/j.1365-2745.2008.01429.x>

2378 Beveridge, C.F., Espinoza, J.-C., Athayde, S., Correa, S.B., Couto, T.B.A., Heilpern, S.A., Jenkins, C.N., Piland, N.C.,
2379 Utsunomiya, R., Wongchuig, S., Anderson, E.P., 2024. The Andes–Amazon–Atlantic pathway: A foundational
2380 hydroclimate system for social–ecological system sustainability. *Proc. Natl. Acad. Sci.* 121, e2306229121.
2381 <https://doi.org/10.1073/pnas.2306229121>

2382 Buras, A., 2017. A comment on the expressed population signal. *Dendrochronologia* 44, 130–132.
2383 <https://doi.org/10.1016/j.dendro.2017.03.005>

2384 Camarero, J.J., Mendivelso, H.A., Sánchez-Salguero, R., 2020. How Past and Future Climate and Drought Drive Radial-
2385 Growth Variability of Three Tree Species in a Bolivian Tropical Dry Forest, in: Pompa-García, M., Camarero, J.J.
2386 (Eds.), *Latin American Dendroecology: Combining Tree-Ring Sciences and Ecology in a Megadiverse Territory*.
2387 Springer International Publishing, Cham, pp. 141–167. https://doi.org/10.1007/978-3-030-36930-9_7

2388 Chavez, S.P., Takahashi, K., 2017. Orographic rainfall hot spots in the Andes–Amazon transition according to the TRMM
2389 precipitation radar and in situ data. *J. Geophys. Res. Atmospheres* 122, 5870–5882.
2390 <https://doi.org/10.1002/2016JD026282>

2391 Cook, E.R., Briffa, K.R., Shiyatov, S., Mazepa, V., 1990. Tree-ring standardization and growth-trend estimation 104–123.

2392 Cook, E.R., Peters, K., 1981. The Smoothing Spline: A New Approach to Standardizing Forest Interior Tree-Ring Width Series
2393 for Dendroclimatic Studies.

2394 Cuesta, F., Tovar, C., Llambí, L.D., Gosling, W.D., Halloy, S., Carilla, J., Muriel, P., Meneses, R.I., Beck, S., Ulloa Ulloa, C.,
2395 Yager, K., Aguirre, N., Viñas, P., Jácome, J., Suárez-Duque, D., Buytaert, W., Pauli, H., 2020. Thermal niche traits
2396 of high alpine plant species and communities across the tropical Andes and their vulnerability to global warming. *J.*
2397 *Biogeogr.* 47, 408–420. <https://doi.org/10.1111/jbi.13759>

2398 Cuyckens, G.A.E., Christie, D.A., Domic, A.I., Malizia, L.R., Renison, D., 2016. Climate change and the distribution and
2399 conservation of the world's highest elevation woodlands in the South American Altiplano. *Glob. Planet. Change* 137,
2400 79–87. <https://doi.org/10.1016/j.gloplacha.2015.12.010>

2401 Cybis Elektronik, 2010. CDendro and Coorecorder [WWW Document]. URL <http://www.cybis.se/forfun/dendro/index.htm>

2402 D'Arrigo, R., Wilson, R., Liepert, B., Cherubini, P., 2008. On the 'Divergence Problem' in Northern Forests: A review of the
2403 tree-ring evidence and possible causes. *Glob. Planet. Change* 60, 289–305.
2404 <https://doi.org/10.1016/j.gloplacha.2007.03.004>

2405 D'Arrigo, R.D., Kaufmann, R.K., Davi, N., Jacoby, G.C., Laskowski, C., Myneni, R.B., Cherubini, P., 2004. Thresholds for
2406 warming-induced growth decline at elevational tree line in the Yukon Territory, Canada. *Glob. Biogeochem. Cycles*
2407 18. <https://doi.org/10.1029/2004GB002249>

2408 Devi, N.M., Kukarskih, V.V., Galimova, A.A., Mazepa, V.S., Grigoriev, A.A., 2020. Climate change evidence in tree growth
2409 and stand productivity at the upper treeline ecotone in the Polar Ural Mountains. *For. Ecosyst.* 7, 7.
2410 <https://doi.org/10.1186/s40663-020-0216-9>

2411 Duque, A., Peña, M.A., Cuesta, F., González-Caro, S., Kennedy, P., Phillips, O.L., Calderón-Loor, M., Blundo, C., Carilla, J.,
2412 Cayola, L., Farfán-Ríos, W., Fuentes, A., Grau, R., Homeier, J., Loza-Rivera, M.I., Malhi, Y., Malizia, A., Malizia,
2413 L., Martínez-Villa, J.A., Myers, J.A., Osinaga-Acosta, O., Peralvo, M., Pinto, E., Saatchi, S., Silman, M., Tello, J.S.,
2414 Terán-Valdez, A., Feeley, K.J., 2021. Mature Andean forests as globally important carbon sinks and future carbon
2415 refuges. *Nat. Commun.* 12, 2138. <https://doi.org/10.1038/s41467-021-22459-8>

- 2416 Enfield, D.B., Mestas-Nuñez, A.M., Mayer, D.A., Cid-Serrano, L., 1999. How ubiquitous is the dipole relationship in tropical
2417 Atlantic sea surface temperatures? *J. Geophys. Res. Oceans* 104, 7841–7848. <https://doi.org/10.1029/1998JC900109>
- 2418 Espinoza, J.-C., Arias, P.A., Moron, V., Junquas, C., Segura, H., Sierra-Pérez, J.P., Wongchuig, S., Condom, T., 2021. Recent
2419 Changes in the Atmospheric Circulation Patterns during the Dry-to-Wet Transition Season in South Tropical South
2420 America (1979–2020): Impacts on Precipitation and Fire Season. *J. Clim.* 34, 9025–9042.
2421 <https://doi.org/10.1175/JCLI-D-21-0303.1>
- 2422 Espinoza, J.C., Ronchail, J., Marengo, J.A., Segura, H., 2019. Contrasting North–South changes in Amazon wet-day and dry-
2423 day frequency and related atmospheric features (1981–2017). *Clim. Dyn.* 52, 5413–5430.
2424 <https://doi.org/10.1007/s00382-018-4462-2>
- 2425 Espinoza, J.C., Segura, H., Ronchail, J., Drapeau, G., Gutierrez-Cori, O., 2016. Evolution of wet-day and dry-day frequency
2426 in the western Amazon basin: Relationship with atmospheric circulation and impacts on vegetation. *Water Resour.*
2427 *Res.* 52, 8546–8560. <https://doi.org/10.1002/2016WR019305>
- 2428 Espinoza, T.E.B., Kessler, M., 2022. A monograph of the genus *Polylepis* (Rosaceae). *PhytoKeys* 203, 1–274.
2429 <https://doi.org/10.3897/phytokeys.203.83529>
- 2430 Feeley, K.J., Rehm, E.M., Machovina, B., 2012. perspective: The responses of tropical forest species to global climate change:
2431 acclimate, adapt, migrate, or go extinct? *Front. Biogeogr.* 4. <https://doi.org/10.21425/F5FBG12621>
- 2432 Feeley, K.J., Silman, M.R., Bush, M.B., Farfan, W., Cabrera, K.G., Malhi, Y., Meir, P., Revilla, N.S., Quisipanqui, M.N.R.,
2433 Saatchi, S., 2011. Upslope migration of Andean trees. *J. Biogeogr.* 38, 783–791. <https://doi.org/10.1111/j.1365-2699.2010.02444.x>
- 2434 Ferrero, M.E., Villalba, R., De Membiela, M., Ripalta, A., Delgado, S., Paolini, L., 2013. Tree-growth responses across
2435 environmental gradients in subtropical Argentinean forests. *Plant Ecol.* 214, 1321–1334.
2436 <https://doi.org/10.1007/s11258-013-0254-2>
- 2437 Finer, M., Mamani, N., 2023. Amazon Deforestation & Fire Hotspots 2022. *MAAP* 187, 2017–21.
- 2438 Flynn, H., Camarero, J.J., Sanmiguel-Vallelado, A., Rojas Heredia, F., Domínguez Aguilar, P., Revuelto, J., López-Moreno,
2439 J.I., 2025. A shift in circadian stem increment patterns in a Pyrenean alpine treeline precedes spring growth after snow
2440 melting. *Biogeosciences* 22, 1135–1147. <https://doi.org/10.5194/bg-22-1135-2025>
- 2441 Frank, D., Esper, J., Cook, E., 2006. On variance adjustments in tree-ring chronology development. *Tree Rings Archaeol.*
2442 *Climatol. Ecol. TRACE* 4, 56–66.
- 2443 Fritts, H.C., 1976. *Tree rings and Climate*. Academic Press, London.
- 2444 Fu, R., Yin, L., Li, W., Arias, P.A., Dickinson, R.E., Huang, L., Chakraborty, S., Fernandes, K., Liebmann, B., Fisher, R.,
2445 Myneni, R.B., 2013. Increased dry-season length over southern Amazonia in recent decades and its implication for
2446 future climate projection. *Proc. Natl. Acad. Sci.* 110, 18110–18115. <https://doi.org/10.1073/pnas.1302584110>
- 2447 Fuentes, A., 2005. Una introducción a la vegetación de la región de Madidi 32.
- 2448 Funk, C., Peterson, P., Landsfeld, M., Pedreros, D., Verdin, J., Shukla, S., Husak, G., Rowland, J., Harrison, L., Hoell, A.,
2449 2015. The climate hazards infrared precipitation with stations—a new environmental record for monitoring extremes.
2450 *Sci. Data* 2, 1–21.
- 2451 García-Núñez, C., Rada, F., Boero, C., González, J., Gallardo, M., Azócar, A., Liberman-Cruz, M., Hilal, M., Prado, F., 2004.
2452 Leaf Gas Exchange and Water Relations in *Polylepis tarapacana* at Extreme Altitudes in the Bolivian Andes.
2453 *Photosynthetica* 42, 133–138. <https://doi.org/10.1023/B:PHOT.0000040581.94641.ed>
- 2454 Garreaud, R., 1999. Multiscale Analysis of the Summertime Precipitation over the Central Andes.
- 2455 Garreaud, R.D., 2009. The Andes climate and weather. *Adv. Geosci.* 22, 3–11. <https://doi.org/10.5194/adgeo-22-3-2009>
- 2456 Good, P., Lowe, J.A., Collins, M., Moufouma-Okia, W., 2008. An objective tropical Atlantic sea surface temperature gradient
2457 index for studies of south Amazon dry-season climate variability and change. *Philos. Trans. R. Soc. B Biol. Sci.* 363,
2458 1761–1766. <https://doi.org/10.1098/rstb.2007.0024>
- 2459 Groenendijk, P., Babst, F., Trouet, V., Fan, Z.-X., Granato-Souza, D., Locosselli, G.M., Mokia, M., Panthi, S., Pumijumnon,
2460 N., Abiyu, A., Acuña-Soto, R., Adenky-Filho, E., Alfaro-Sánchez, R., Anholletto Junior, C.R., Aragão, J.R.V.,
2461 Assis-Pereira, G., Astudillo-Sánchez, C.C., Carolina Barbosa, A., Barreto, N. de O., Battipaglia, G., Beeckman, H.,
2462 Botosso, P.C., Bourland, N., Bräuning, A., Brienen, R., Brookhouse, M., Buajan, S., Buckley, B.M., Camarero, J.J.,
2463 Carrillo-Parra, A., Ceccantini, G., Centeno-Erguera, L.R., Cerano-Paredes, J., Cervantes-Martínez, R., Chanthorn,
2464 W., Chen, Y.-J., Cintra, B.B.L., Comejo-Oviedo, E.H., Cortés-Cortés, O., Costa, C.M., Couralet, C., Crispin-

2466 DelaCruz, D.B., D'Arrigo, R., David, D.A., De Ridder, M., Del Valle, J.I., Diaz-Carrillo, O.A., Dobner Jr, M., Doucet,
2467 J.-L., Dünisch, O., Enquist, B.J., Esemann-Quadros, K., Esquivel-Arriaga, G., Fayolle, A., Fenilli, T.A.B., Ferrero,
2468 M.E., Fichtler, E., Finnegan, P.M., Fontana, C., Francisco, K.S., Fu, P.-L., Galvão, F., Gebrekirstos, A., Giraldo, J.A.,
2469 Gloor, E., Godoy-Veiga, M., Guerra, A., Haneca, K., Harley, G.L., Heinrich, I., Helle, G., Hernández-Díaz, J.C.,
2470 Hornink, B., Hubau, W., Inga, J.G., Islam, M., Jiang, Y., Kaib, M., Hassan Khamisi, Z., Koprowski, M., Layme, E.,
2471 Leffler, A.J., Ligot, G., Lisi, C.S., Loader, N.J., Lobo, F. de A., Longhi-Santos, T., Lopez, L., López-Hernández, M.I.,
2472 Lousada, J.L.P.C., Manzanedo, R.D., Marcon, A.K., Maxwell, J.T., Mendivelso, H.A., Mendoza-Villa, O.N.,
2473 Menezes, Í.R.N., Montóia, V.R., Moors, E., Moreno, M., Muñoz-Castro, M.A., Nabais, C., Nathalang, A., Ngoma, J.,
2474 Nogueira Jr., F. de C., Oliveira, J.M., Olmedo, G.M., Ortega-Rodríguez, D.R., Ortiz, C.E.R., Pagotto, M.A., Paredes-
2475 Villanueva, K., Pérez-De-Lis, G., Ponce Calderón, L.P., Portal-Cahuana, L.A., Pucha-Cofrep, D.A., Quadri, P.,
2476 Rahman, M., Ramírez, J.A., Requena-Rojas, E.J., Reyes-Flores, J., Ribeiro, A. de S., Robertson, I., Roig, F.A.,
2477 Roquette, J.G., Rubio-Camacho, E.A., Sánchez-Salguero, R., Sass-Klaassen, U., Schöngart, J., Scipioni, M.C.,
2478 Sheppard, P.R., Silva, L.C.R., Slotta, F., Soria-Díaz, L., Sousa, L.K.V.S., Speer, J.H., Therrell, M.D., Ticse-Otarola,
2479 G., Tomazello-Filho, M., Torbenson, M.C.A., Tor-Ngern, P., Touchan, R., Van Den Bulcke, J., Vázquez-Selem, L.,
2480 Velázquez-Pérez, A.H., Venegas-González, A., Villalba, R., Villanueva-Díaz, J., Vlam, M., Vourlitis, G., Wehenkel,
2481 C., Wils, T., Zavaleta, E.S., Zewdu, E.A., Zhang, Y.-J., Zhou, Z.-K., Zuidema, P.A., 2025. The importance of tropical
2482 tree-ring chronologies for global change research. *Quat. Sci. Rev.* 355, 109233.
2483 <https://doi.org/10.1016/j.quascirev.2025.109233>

2484 Harris, I., Osborn, T.J., Jones, P., Lister, D., 2020. Version 4 of the CRU TS monthly high-resolution gridded multivariate
2485 climate dataset. *Sci. Data* 7, 109. <https://doi.org/10.1038/s41597-020-0453-3>

2486 Haurwitz, M.W., Brier, G.W., 1981. A critique of the superposed epoch analysis method: its application to solar-weather
2487 relations. *Mon. Weather Rev.* 109, 2074–2079.

2488 Hertel, D., Wesche, K., 2008. Tropical moist Polylepis stands at the treeline in East Bolivia: the effect of elevation on stand
2489 microclimate, above- and below-ground structure, and regeneration. *Trees* 22, 303–315.
2490 <https://doi.org/10.1007/s00468-007-0185-4>

2491 Hoch, G., Körner, C., 2005. Growth, Demography and Carbon Relations of Polylepis Trees at the World's Highest Treeline.
2492 *Funct. Ecol.* 19, 941–951.

2493 Hock, R., Rasul, G., Adler, C., Caceres, B., Gruber, S., Hirabayashi, Y., Jackson, M., Kääb, A., Kang, S., Kutuzov, S., Milner,
2494 A., Molau, U., Morin, S., Orlove, B., Steltzer, H., Allen, S., Arenson, L., Banerjee, S., Barr, I., Bórquez, R., Brown,
2495 L., Cao, B., Carey, M., Cogley, G., Fischlin, A., A de Sherbinin, Eckert, N., Geertsema, M., Hagenstad, M., Honsberg,
2496 M., Hood, E., Huss, M., E Jimenez Zamora, Kotlarski, S., Lefevre, P., J Ignacio López Moreno, Lundquist, J.,
2497 Mcdowell, G., Mills, S., Mou, C., Nepal, S., Noetzli, J., Palazzi, E., Pepin, N., Rixen, C., Shahgedanova, M., S
2498 McKenzie Skiles, Vincent, C., Viviroli, D., Gesa, A.W., P Yangjee Sherpa, Weyer, N., Wouters, B., Yasunari, T.,
2499 You, Q., Zhang, Y., 2019. High Mountain Areas. STATI UNITI D'AMERICA.

2500 Hoffmann, D., Weggenmann, D., 2013. Climate Change Induced Glacier Retreat and Risk Management: Glacial Lake Outburst
2501 Floods (GLOFs) in the Apolobamba Mountain Range, Bolivia, in: Leal Filho, W. (Ed.), *Climate Change and Disaster
2502 Risk Management, Climate Change Management*. Springer, Berlin, Heidelberg, pp. 71–87.
2503 https://doi.org/10.1007/978-3-642-31110-9_5

2504 Hua, Q., Turnbull, J.C., Santos, G.M., Rakowski, A.Z., Ancapichún, S., Pol-Holz, R.D., Hammer, S., Lehman, S.J., Levin, I.,
2505 Miller, J.B., Palmer, J.G., Turney, C.S.M., 2022. ATMOSPHERIC RADIOCARBON FOR THE PERIOD 1950–
2506 2019. *Radiocarbon* 64, 723–745. <https://doi.org/10.1017/RDC.2021.95>

2507 Jacoby, G.C., D'Arrigo, R.D., 1995. Tree ring width and density evidence of climatic and potential forest change in Alaska.
2508 *Glob. Biogeochem. Cycles* 9, 227–234. <https://doi.org/10.1029/95GB00321>

2509 Jaramillo, A.D., 2015. Fotosíntesis en los Bosques a Mayor Elevación en el Planeta: Polylepis tarapacana en un Gradiente de
2510 Elevación en los Andes de Arica y Parinacota, Chile.

2511 Jomelli, V., Pavlova, I., Guin, O., Soliz-Gamboa, C., Contreras, A., Toivonen, J.M., Zetterberg, P., 2012. Analysis of the
2512 Dendroclimatic Potential of Polylepis pepei, P. subsericans and P. rugulosa In the Tropical Andes (Peru-Bolivia).
2513 *Tree-Ring Res.* 68, 91–103. <https://doi.org/10.3959/2011-10.1>

2514 Junquas, C., Takahashi, K., Condom, T., Espinoza, J.-C., Chavez, S., Sicart, J.-E., Lebel, T., 2018. Understanding the influence
2515 of orography on the precipitation diurnal cycle and the associated atmospheric processes in the central Andes. *Clim.*
2516 *Dyn.* 50, 3995–4017. <https://doi.org/10.1007/s00382-017-3858-8>

2517 Kessler, M., Toivonen, J.M., Sylvester, S.P., Kluge, J., Hertel, D., 2014. Elevational patterns of *Polylepis* tree height
2518 (Rosaceae) in the high Andes of Peru: role of human impact and climatic conditions. *Front. Plant Sci.* 5.
2519 <https://doi.org/10.3389/fpls.2014.00194>

2520 Kolmogorov, A., 1933. Sulla determinazione empirica di una legge di distribuzione. *Giorn. Dell'ist. Ital. Degli Atti* 4, 89–91.

2521 Körner, C., 2012. Definitions and conventions, in: Körner, C. (Ed.), *Alpine Treelines: Functional Ecology of the Global High*
2522 *Elevation Tree Limits*. Springer, Basel, pp. 11–19. https://doi.org/10.1007/978-3-0348-0396-0_2

2523 Körner, C., Hoch, G., 2023. Not every high-latitude or high-elevation forest edge is a treeline. *J. Biogeogr.* 50, 838–845.
2524 <https://doi.org/10.1111/jbi.14593>

2525 Locosselli, G.M., Brienen, R.J.W., Leite, M. de S., Gloor, M., Krottenthaler, S., Oliveira, A.A. de, Barichivich, J., Anhof, D.,
2526 Ceccantini, G., Schöngart, J., Buckeridge, M., 2020. Global tree-ring analysis reveals rapid decrease in tropical tree
2527 longevity with temperature. *Proc. Natl. Acad. Sci.* 117, 33358–33364. <https://doi.org/10.1073/pnas.2003873117>

2528 López, V.L., Huertas Herrera, A., Rosas, Y.M., Cellini, J.M., 2022. Optimal environmental drivers of high-mountains forest:
2529 *Polylepis tarapacana* cover evaluation in their southernmost distribution range of the Andes. *Trees For. People* 9,
2530 100321. <https://doi.org/10.1016/j.tfp.2022.100321>

2531 Macek, P., Macková, J., de Bello, F., 2009. Morphological and ecophysiological traits shaping altitudinal distribution of three
2532 *Polylepis* treeline species in the dry tropical Andes. *Acta Oecologica* 35, 778–785.
2533 <https://doi.org/10.1016/j.actao.2009.08.013>

2534 Macía, M.J., 2008. Woody plants diversity, floristic composition and land use history in the Amazonian rain forests of Madidi
2535 National Park, Bolivia. *Biodivers. Conserv.* 17, 2671–2690. <https://doi.org/10.1007/s10531-008-9348-x>

2536 Malhi, Y., Roberts, J.T., Betts, R.A., Killeen, T.J., Li, W., Nobre, C.A., 2008. Climate Change, Deforestation, and the Fate of
2537 the Amazon. *Science* 319, 169–172.

2538 Malizia, A., Blundo, C., Carilla, J., Acosta, O.O., Cuesta, F., Duque, A., Aguirre, N., Aguirre, Z., Ataroff, M., Baez, S.,
2539 Calderón-Loor, M., Cayola, L., Cayuela, L., Ceballos, S., Cedillo, H., Ríos, W.F., Feeley, K.J., Fuentes, A.F., Álvarez,
2540 L.E.G., Grau, R., Homeier, J., Jadan, O., Llambi, L.D., Rivera, M.I.L., Macía, M.J., Malhi, Y., Malizia, L., Peralvo,
2541 M., Pinto, E., Tello, S., Silman, M., Young, K.R., 2020. Elevation and latitude drives structure and tree species
2542 composition in Andean forests: Results from a large-scale plot network. *PLOS ONE* 15, e0231553.
2543 <https://doi.org/10.1371/journal.pone.0231553>

2544 Marengo, J.A., Tomasella, J., Alves, L.M., Soares, W.R., Rodriguez, D.A., 2011. The drought of 2010 in the context of
2545 historical droughts in the Amazon region. *Geophys. Res. Lett.* 38. <https://doi.org/10.1029/2011GL047436>

2546 Meko, D.M., Touchan, R., Anchukaitis, K.J., 2011. Seascorr: A MATLAB program for identifying the seasonal climate signal
2547 in an annual tree-ring time series. *Comput. Geosci.* 37, 1234–1241. <https://doi.org/10.1016/j.cageo.2011.01.013>

2548 Melvin, T., 2004. Historical growth rates and changing climatic sensitivity of boreal conifers.

2549 Montaña-Centellas, F., Fuentes, A.F., Cayola, L., Macía, M.J., Arellano, G., Loza, M.I., Nieto-Ariza, B., Tello, J.S., 2024.
2550 Elevational range sizes of woody plants increase with climate variability in the Tropical Andes. *J. Biogeogr.* 51, 814–
2551 826. <https://doi.org/10.1111/jbi.14783>

2552 Morales, M.S., Crispín-DelaCruz, D.B., Álvarez, C., Christie, D.A., Ferrero, M.E., Andreu-Hayles, L., Villalba, R., Guerra,
2553 A., Ticse-Otarola, G., Rodríguez-Ramírez, E.C., LLoclla-Martínez, R., Sanchez-Ferrer, J., Requena-Rojas, E.J.,
2554 2023. Drought increase since the mid-20th century in the northern South American Altiplano revealed by a 389-year
2555 precipitation record. *Clim. Past* 19, 457–476. <https://doi.org/10.5194/cp-19-457-2023>

2556 Morales, M.S., Villalba, R., Grau, H.R., Paolini, L., 2004. Rainfall-Controlled Tree Growth in High-Elevation Subtropical
2557 Treelines. *Ecology* 85, 3080–3089. <https://doi.org/10.1890/04-0139>

2558 Muller, M.R., 2017. Protected areas and their relationship with food security in a context of climate change: an overview from
2559 Bolivia, Brazil and Peru. *Prot. AREAS*.

2560 Navarro, G., Arrázola, S., Balderrama, J.A., Ferreira, W., De la Barra, N., Antezana, C., Gómez, I., Mercado, M., 2010.
2561 Diagnóstico del estado de conservación y caracterización de los bosques de *Polylepis* en Bolivia y su avifauna
2562 Conservation state analysis and characterization of the Bolivian *Polylepis* forests and their avifauna. *Rev. Boliv. Ecol.*
2563 *Conserv. Ambient.* 28, 1–35.

2564 Oelkers, R.C., Andreu-Hayles, L., D'Arrigo, R., Pacheco-Solana, A., Rodriguez-Caton, M., Fuentes, A., Santos, G.M.,
2565 Tejedor, E., Ferrero, M.E., Maldonado, C., 2023. Recent growth increase in endemic *Juglans boliviana* from the
2566 tropical Andes. *Dendrochronologia* 79, 126090. <https://doi.org/10.1016/j.dendro.2023.126090>

2567 Paegle, J.N., Mo, K.C., 2002. Linkages between Summer Rainfall Variability over South America and Sea Surface
2568 Temperature Anomalies.

2569 Paulsen, J., Weber, U. M., and Körner, Ch., 2000. Tree Growth near Treeline: Abrupt or Gradual Reduction with Altitude?
2570 *Arct. Antarct. Alp. Res.* 32, 14–20. <https://doi.org/10.1080/15230430.2000.12003334>

2571 Pettitt, A.N., 1979. A Non-Parametric Approach to the Change-Point Problem. *J. R. Stat. Soc. Ser. C Appl. Stat.* 28, 126–135.
2572 <https://doi.org/10.2307/2346729>

2573 Quesada-Román, A., Ballesteros-Cánovas, J.A., St. George, S., Stoffel, M., 2022. Tropical and subtropical dendrochronology:
2574 Approaches, applications, and prospects. *Ecol. Indic.* 144, 109506. <https://doi.org/10.1016/j.ecolind.2022.109506>

2575 Rao, M.P., Cook, E.R., Cook, B.I., Anchukaitis, K.J., D'Arrigo, R.D., Krusic, P.J., LeGrande, A.N., 2019. A double bootstrap
2576 approach to Superposed Epoch Analysis to evaluate response uncertainty. *Dendrochronologia* 55, 119–124.
2577 <https://doi.org/10.1016/j.dendro.2019.05.001>

2578 Rasmusson, E.M., Carpenter, T.H., 1982. Variations in tropical sea surface temperature and surface wind fields associated
2579 with the Southern Oscillation/El Niño. *Mon. Weather Rev.* 110, 354–384.

2580 Rehm, E.M., Feeley, K.J., 2013. Forest patches and the upward migration of timberline in the southern Peruvian Andes. *For.*
2581 *Ecol. Manag.* 305, 204–211. <https://doi.org/10.1016/j.foreco.2013.05.041>

2582 Requena-Rojas, E.J., Amoroso, M.M., Ticse-Otarola, G., Crispin-Delacruz, D.B., 2021. Assessing Dendrochronological
2583 Potential of *Escallonia myrtilloides* in the High Andes of Peru. *Tree-Ring Res.* 77, 41–52.
2584 <https://doi.org/10.3959/TRR2019-8>

2585 Requena-Rojas, E.J., Crispin-DelaCruz, D.B., Ticse-Otarola, G., Quispe-Melgar, H.R., Inga Guillen, J.G., Camel Paucar, V.,
2586 Guerra, A., Ames-Martinez, F.N., Morales, M., 2020. Temporal Growth Variation in High-Elevation Forests: Case
2587 Study of *Polylepis* Forests in Central Andes, in: Pompa-García, M., Camarero, J.J. (Eds.), *Latin American*
2588 *Dendroecology: Combining Tree-Ring Sciences and Ecology in a Megadiverse Territory*. Springer International
2589 Publishing, Cham, pp. 263–279. https://doi.org/10.1007/978-3-030-36930-9_12

2590 Roig, F., Fernández, M., Gareca León, E., Altamirano, S., Monge, S., 2001. ESTUDIOS DENDROCRONOLÓGICOS EN
2591 LOS AMBIENTES HÚMEDOS DE LA PUNA BOLIVIANA DENDROCHRONOLOGICAL STUDIES IN THE
2592 HUMID PUNA ENVIRONMENTS OF BOLIVIA. *Rev Bol Ecol* 9.

2593 Rolland, C., Petitcolas, V., Michalet, R., 1998. Changes in radial tree growth for *Picea abies*, *Larix decidua*, *Pinus cembra* and
2594 *Pinus uncinata* near the alpine timberline since 1750. *Trees* 13, 40–53. <https://doi.org/10.1007/PL00009736>

2595 Romatschke, U., Houze, R.A., 2010. Extreme Summer Convection in South America. <https://doi.org/10.1175/2010JCLI3465.1>

2596 Ronchaill, J., Espinoza, J.C., Drapeau, G., Sabot, M., Cochonneau, G., Schor, T., 2018. The flood recession period in Western
2597 Amazonia and its variability during the 1985–2015 period. *J. Hydrol. Reg. Stud.* 15, 16–30.
2598 <https://doi.org/10.1016/j.ejrh.2017.11.008>

2599 Ropelewski, C.F., Halpert, M.S., 1987. Global and Regional Scale Precipitation Patterns Associated with the El Niño/Southern
2600 Oscillation.

2601 Schulman, E., 1956. *Dendroclimatic Changes in Semiarid America*. University of Arizona Press, Tucson, p. 142.

2602 Segura, H., Espinoza, J.C., Junquas, C., Lebel, T., Vuille, M., Condom, T., 2022. Extreme austral winter precipitation events
2603 over the South-American Altiplano: regional atmospheric features. *Clim. Dyn.* 59, 3069–3086.
2604 <https://doi.org/10.1007/s00382-022-06240-1>

2605 Sierra, J.P., Junquas, C., Espinoza, J.C., Segura, H., Condom, T., Andrade, M., Molina-Carpio, J., Ticona, L., Mardoñez, V.,
2606 Blacutt, L., Polcher, J., Rabatel, A., Sicart, J.E., 2022. Deforestation impacts on Amazon-Andes hydroclimatic
2607 connectivity. *Clim. Dyn.* 58, 2609–2636. <https://doi.org/10.1007/s00382-021-06025-y>

2608 Simpson, B.B., 1979. A revision of the genus *Polylepis* (Rosaceae: Sanguisorbeae). *Smithson. Contrib. Bot.*

2609 Smirnov, N., 1948. Table for estimating the goodness of fit of empirical distributions. *Ann. Math. Stat.* 19, 279–281.

2610 Srur, A.M., Villalba, R., Rodríguez-Catón, M., Amoroso, M.M., Marcotti, E., 2018. Climate and *Nothofagus pumilio*
2611 Establishment at Upper Treelines in the Patagonian Andes. *Front. Earth Sci.* 6.
2612 <https://doi.org/10.3389/feart.2018.00057>

2613 Srur, A.M., Villalba ,Ricardo, Rodríguez-Catón ,Milagros, Amoroso ,Mariano M., and Marcotti, E., 2016. Establishment of
2614 *Nothofagus pumilio* at Upper Treelines Across a Precipitation Gradient in the Northern Patagonian Andes. *Arct.*
2615 *Antarct. Alp. Res.* 48, 755–766. <https://doi.org/10.1657/AAAR0016-015>
2616 Stokes, M.A., Smiley, T.L., 1968. An introduction to tree-ring dating. University of Chicago Press, Chicago, Illinois.
2617 Thompson, L.G., Mosley-Thompson, E., Brecher, H., Davis, M., León, B., Les, D., Lin, P.-N., Mashiotta, T., Mountain, K.,
2618 2006. Abrupt tropical climate change: Past and present. *Proc. Natl. Acad. Sci.* 103, 10536–10543.
2619 <https://doi.org/10.1073/pnas.0603900103>
2620 Tovar, C., Carril, A.F., Gutiérrez, A.G., Ahrends, A., Fita, L., Zaninelli, P., Flombaum, P., Abarzúa, A.M., Alarcón, D.,
2621 Aschero, V., Báez, S., Barros, A., Carilla, J., Ferrero, M.E., Flantua, S.G.A., González, P., Menéndez, C.G., Pérez-
2622 Escobar, O.A., Pauchard, A., Ruscica, R.C., Särkinen, T., Sörensson, A.A., Srur, A., Villalba, R., Hollingsworth,
2623 P.M., 2022. Understanding climate change impacts on biome and plant distributions in the Andes: Challenges and
2624 opportunities. *J. Biogeogr.* 49, 1420–1442. <https://doi.org/10.1111/jbi.14389>
2625 Vera, C., Higgins, W., Amador, J., Ambrizzi, T., Garreaud, R., Gochis, D., Gutzler, D., Lettenmaier, D., Marengo, J., Mechoso,
2626 C.R., Noguez-Paele, J., Silva Dias, P.L., Zhang, C., 2006. Toward a Unified View of the American Monsoon
2627 Systems. *J. Clim.* 19, 4977–5000. <https://doi.org/10.1175/JCLI3896.1>
2628 Virtanen, P., Gommers, R., Oliphant, T.E., Haberland, M., Reddy, T., Cournapeau, D., Burovski, E., Peterson, P., Weckesser,
2629 W., Bright, J., 2020. SciPy 1.0: fundamental algorithms for scientific computing in Python. *Nat. Methods* 17, 261–
2630 272.
2631 von Arx, G., Crivellaro, A., Prendin, A.L., Čufar, K., Carrer, M., 2016. Quantitative Wood Anatomy—Practical Guidelines.
2632 *Front. Plant Sci.* 7.
2633 Vuille, M., Bradley, R.S., Keimig, F., 2000. Interannual climate variability in the Central Andes and its relation to tropical
2634 Pacific and Atlantic forcing. *J. Geophys. Res. Atmospheres* 105, 12447–12460.
2635 <https://doi.org/10.1029/2000JD900134>
2636 Waskom, M.L., 2021. seaborn: statistical data visualization. *J. Open Source Softw.* 6, 3021.
2637 <https://doi.org/10.21105/joss.03021>
2638 Wigley, T.M.L., Briffa, K.R., Jones, P.D., 1984. On the Average Value of Correlated Time Series, with Applications in
2639 Dendroclimatology and Hydrometeorology. *J. Appl. Meteorol. Climatol.* 23, 201–213. [https://doi.org/10.1175/1520-0450\(1984\)023<0201:OTAVOC>2.0.CO;2](https://doi.org/10.1175/1520-0450(1984)023<0201:OTAVOC>2.0.CO;2)
2640 Wilmking, M., D'Arrigo, R., Jacoby, G.C., Juday, G.P., 2005. Increased temperature sensitivity and divergent growth trends
2641 in circumpolar boreal forests. *Geophys. Res. Lett.* 32. <https://doi.org/10.1029/2005GL023331>
2642 Wolter, K., Timlin, M.S., 2011. El Niño/Southern Oscillation behaviour since 1871 as diagnosed in an extended multivariate
2643 ENSO index (MEI.ext). *Int. J. Climatol.* 31, 1074–1087. <https://doi.org/10.1002/joc.2336>
2644 Yoon, J., Zeng, N., 2010. An Atlantic influence on Amazon rainfall. *Clim. Dyn.* 34, 249–264. <https://doi.org/10.1007/s00382-009-0551-6>
2645 Young, K.R., León, B., 2006. Tree-line changes along the Andes: implications of spatial patterns and dynamics. *Philos. Trans.*
2646 *R. Soc. B Biol. Sci.* 362, 263–272. <https://doi.org/10.1098/rstb.2006.1986>
2647 Zang, C., Biondi, F., 2015. treeclim: an R package for the numerical calibration of proxy-climate relationships. *Ecography* 38,
2648 431–436. <https://doi.org/10.1111/ecog.01335>
2649 Zanin, P.R., Satyamurty, P., 2020. Hydrological processes interconnecting the two largest watersheds of South America from
2650 multi-decadal to inter-annual time scales: A critical review. *Int. J. Climatol.* 40, 4006–4038.
2651 <https://doi.org/10.1002/joc.6442>
2652 Zapata, F., 2013. A multilocus phylogenetic analysis of *Escallonia* (Escalloniaceae): Diversification in montane South
2653 America. *Am. J. Bot.* 100, 526–545. <https://doi.org/10.3732/ajb.1200297>

Page 1: [1] Formatted	Rose Oelkers	11/24/25 11:43:00 PM
------------------------------	---------------------	-----------------------------

Font: 12 pt

Page 1: [1] Formatted	Rose Oelkers	11/24/25 11:43:00 PM
------------------------------	---------------------	-----------------------------

Font: 12 pt

Page 1: [1] Formatted	Rose Oelkers	11/24/25 11:43:00 PM
------------------------------	---------------------	-----------------------------

Font: 12 pt

Page 1: [1] Formatted	Rose Oelkers	11/24/25 11:43:00 PM
------------------------------	---------------------	-----------------------------

Font: 12 pt

Page 1: [2] Formatted	Rose Oelkers	11/24/25 11:43:00 PM
------------------------------	---------------------	-----------------------------

Font: 12 pt

Page 1: [2] Formatted	Rose Oelkers	11/24/25 11:43:00 PM
------------------------------	---------------------	-----------------------------

Font: 12 pt

Page 1: [2] Formatted	Rose Oelkers	11/24/25 11:43:00 PM
------------------------------	---------------------	-----------------------------

Font: 12 pt

Page 1: [3] Deleted	Rose Oelkers	11/24/25 11:43:00 PM
----------------------------	---------------------	-----------------------------

▼

Page 1: [4] Formatted	Rose Oelkers	11/24/25 11:43:00 PM
------------------------------	---------------------	-----------------------------

Left, No bullets or numbering

Page 1: [5] Formatted	Rose Oelkers	11/24/25 11:43:00 PM
------------------------------	---------------------	-----------------------------

Font: 10 pt

Page 1: [5] Formatted	Rose Oelkers	11/24/25 11:43:00 PM
------------------------------	---------------------	-----------------------------

Font: 10 pt

Page 1: [6] Formatted	Rose Oelkers	11/24/25 11:43:00 PM
------------------------------	---------------------	-----------------------------

Font: 10 pt

Page 1: [6] Formatted	Rose Oelkers	11/24/25 11:43:00 PM
------------------------------	---------------------	-----------------------------

Font: 10 pt

Page 1: [7] Formatted	Rose Oelkers	11/24/25 11:43:00 PM
------------------------------	---------------------	-----------------------------

Font: 10 pt

Page 1: [8] Formatted	Rose Oelkers	11/24/25 11:43:00 PM
------------------------------	---------------------	-----------------------------

Font: 10 pt

Page 1: [9] Formatted	Rose Oelkers	11/24/25 11:43:00 PM
------------------------------	---------------------	-----------------------------

Font: 10 pt

Page 1: [10] Formatted	Rose Oelkers	11/24/25 11:43:00 PM
-------------------------------	---------------------	-----------------------------

Font: 10 pt

Page 1: [11] Formatted	Rose Oelkers	11/24/25 11:43:00 PM
-------------------------------	---------------------	-----------------------------

Font: 10 pt

Page 1: [11] Formatted	Rose Oelkers	11/24/25 11:43:00 PM
-------------------------------	---------------------	-----------------------------

Font: 10 pt

Page 1: [12] Formatted	Rose Oelkers	11/24/25 11:43:00 PM
-------------------------------	---------------------	-----------------------------

Font: 10 pt

Page 1: [13] Formatted	Rose Oelkers	11/24/25 11:43:00 PM
-------------------------------	---------------------	-----------------------------

Font: 10 pt

Page 1: [14] Formatted	Rose Oelkers	11/24/25 11:43:00 PM
-------------------------------	---------------------	-----------------------------

Font: 10 pt

Page 1: [15] Formatted	Rose Oelkers	11/24/25 11:43:00 PM
-------------------------------	---------------------	-----------------------------

Font: 10 pt

Page 1: [16] Formatted	Rose Oelkers	11/24/25 11:43:00 PM
-------------------------------	---------------------	-----------------------------

Spanish

Page 1: [17] Formatted	Rose Oelkers	11/24/25 11:43:00 PM
-------------------------------	---------------------	-----------------------------

Left, Space Before: 0 pt

Page 1: [18] Deleted	Rose Oelkers	11/24/25 11:43:00 PM
-----------------------------	---------------------	-----------------------------

▼

Page 1: [19] Formatted	Rose Oelkers	11/24/25 11:43:00 PM
-------------------------------	---------------------	-----------------------------

Font color: Text 1

Page 1: [20] Formatted	Rose Oelkers	11/24/25 11:43:00 PM
-------------------------------	---------------------	-----------------------------

Font color: Text 1

Page 1: [21] Formatted	Rose Oelkers	11/24/25 11:43:00 PM
-------------------------------	---------------------	-----------------------------

Font color: Text 1

Page 1: [21] Formatted	Rose Oelkers	11/24/25 11:43:00 PM
-------------------------------	---------------------	-----------------------------

Font color: Text 1

Page 1: [22] Deleted	Rose Oelkers	11/24/25 11:43:00 PM
-----------------------------	---------------------	-----------------------------

▼

Page 1: [22] Deleted	Rose Oelkers	11/24/25 11:43:00 PM
-----------------------------	---------------------	-----------------------------

▼

Page 1: [22] Deleted	Rose Oelkers	11/24/25 11:43:00 PM
-----------------------------	---------------------	-----------------------------

▼

Page 1: [22] Deleted	Rose Oelkers	11/24/25 11:43:00 PM
-----------------------------	---------------------	-----------------------------

▼

Page 1: [22] Deleted	Rose Oelkers	11/24/25 11:43:00 PM
-----------------------------	---------------------	-----------------------------

▼

Page 1: [22] Deleted	Rose Oelkers	11/24/25 11:43:00 PM
-----------------------------	---------------------	-----------------------------

▼

Page 1: [22] Deleted	Rose Oelkers	11/24/25 11:43:00 PM
-----------------------------	---------------------	-----------------------------

▼

Page 1: [22] Deleted	Rose Oelkers	11/24/25 11:43:00 PM
-----------------------------	---------------------	-----------------------------

▼

Page 1: [22] Deleted	Rose Oelkers	11/24/25 11:43:00 PM
-----------------------------	---------------------	-----------------------------

▼

Page 1: [22] Deleted	Rose Oelkers	11/24/25 11:43:00 PM
-----------------------------	---------------------	-----------------------------

▼

Page 1: [22] Deleted	Rose Oelkers	11/24/25 11:43:00 PM
-----------------------------	---------------------	-----------------------------

▼

Page 1: [22] Deleted	Rose Oelkers	11/24/25 11:43:00 PM
-----------------------------	---------------------	-----------------------------

▼

Page 1: [22] Deleted	Rose Oelkers	11/24/25 11:43:00 PM
-----------------------------	---------------------	-----------------------------

▼

Page 1: [22] Deleted	Rose Oelkers	11/24/25 11:43:00 PM
-----------------------------	---------------------	-----------------------------

Page 8: [49] Deleted **Rose Oelkers** **11/24/25 11:43:00 PM**

▼

Page 8: [49] Deleted **Rose Oelkers** **11/24/25 11:43:00 PM**

▼

Page 8: [49] Deleted **Rose Oelkers** **11/24/25 11:43:00 PM**

▼

Page 10: [50] Deleted **Rose Oelkers** **11/24/25 11:43:00 PM**

Page 12: [51] Deleted **Rose Oelkers** **11/24/25 11:43:00 PM**

Page 12: [52] Formatted **Rose Oelkers** **11/24/25 11:43:00 PM**

Font: 10 pt

Page 12: [53] Formatted **Rose Oelkers** **11/24/25 11:43:00 PM**

Font: 10 pt

Page 12: [53] Formatted **Rose Oelkers** **11/24/25 11:43:00 PM**

Font: 10 pt

Page 12: [53] Formatted **Rose Oelkers** **11/24/25 11:43:00 PM**

Font: 10 pt

Page 12: [54] Formatted **Rose Oelkers** **11/24/25 11:43:00 PM**

Font: 10 pt

Page 12: [54] Formatted **Rose Oelkers** **11/24/25 11:43:00 PM**

Font: 10 pt

Page 12: [54] Formatted **Rose Oelkers** **11/24/25 11:43:00 PM**

Font: 10 pt

Page 12: [55] Formatted **Rose Oelkers** **11/24/25 11:43:00 PM**

Font: 10 pt

Page 12: [55] Formatted **Rose Oelkers** **11/24/25 11:43:00 PM**

Font: 10 pt

Page 12: [55] Formatted **Rose Oelkers** **11/24/25 11:43:00 PM**

Font: 10 pt

Page 12: [56] Formatted	Rose Oelkers	11/24/25 11:43:00 PM
--------------------------------	---------------------	-----------------------------

Font: 10 pt

Page 12: [57] Formatted	Rose Oelkers	11/24/25 11:43:00 PM
--------------------------------	---------------------	-----------------------------

Font: 10 pt, Font color: Auto

Page 12: [57] Formatted	Rose Oelkers	11/24/25 11:43:00 PM
--------------------------------	---------------------	-----------------------------

Font: 10 pt, Font color: Auto

Page 12: [58] Formatted	Rose Oelkers	11/24/25 11:43:00 PM
--------------------------------	---------------------	-----------------------------

Font: 10 pt

Page 12: [59] Formatted	Rose Oelkers	11/24/25 11:43:00 PM
--------------------------------	---------------------	-----------------------------

Font: 10 pt, Font color: Black

Page 12: [59] Formatted	Rose Oelkers	11/24/25 11:43:00 PM
--------------------------------	---------------------	-----------------------------

Font: 10 pt, Font color: Black

Page 12: [60] Formatted	Rose Oelkers	11/24/25 11:43:00 PM
--------------------------------	---------------------	-----------------------------

Font: 10 pt

Page 12: [61] Formatted	Rose Oelkers	11/24/25 11:43:00 PM
--------------------------------	---------------------	-----------------------------

Font: 10 pt

Page 12: [61] Formatted	Rose Oelkers	11/24/25 11:43:00 PM
--------------------------------	---------------------	-----------------------------

Font: 10 pt

Page 12: [62] Formatted	Rose Oelkers	11/24/25 11:43:00 PM
--------------------------------	---------------------	-----------------------------

Font: 10 pt

Page 12: [63] Formatted	Rose Oelkers	11/24/25 11:43:00 PM
--------------------------------	---------------------	-----------------------------

Font: 10 pt

Page 12: [64] Formatted	Rose Oelkers	11/24/25 11:43:00 PM
--------------------------------	---------------------	-----------------------------

Font: 10 pt

Page 12: [64] Formatted	Rose Oelkers	11/24/25 11:43:00 PM
--------------------------------	---------------------	-----------------------------

Font: 10 pt

Page 12: [65] Formatted	Rose Oelkers	11/24/25 11:43:00 PM
--------------------------------	---------------------	-----------------------------

Font: 10 pt

Page 12: [65] Formatted	Rose Oelkers	11/24/25 11:43:00 PM
--------------------------------	---------------------	-----------------------------

Page 15: [79] Deleted **Rose Oelkers** **11/24/25 11:43:00 PM**

▼

Page 15: [80] Formatted **Rose Oelkers** **11/24/25 11:43:00 PM**

Font: 10 pt

Page 15: [80] Formatted **Rose Oelkers** **11/24/25 11:43:00 PM**

Font: 10 pt

Page 15: [80] Formatted **Rose Oelkers** **11/24/25 11:43:00 PM**

Font: 10 pt

Page 15: [81] Formatted **Rose Oelkers** **11/24/25 11:43:00 PM**

Font: 10 pt

Page 15: [81] Formatted **Rose Oelkers** **11/24/25 11:43:00 PM**

Font: 10 pt

Page 15: [81] Formatted **Rose Oelkers** **11/24/25 11:43:00 PM**

Font: 10 pt

Page 15: [82] Deleted **Rose Oelkers** **11/24/25 11:43:00 PM**

▼

Page 15: [83] Deleted **Rose Oelkers** **11/24/25 11:43:00 PM**

▼

Page 15: [84] Deleted **Rose Oelkers** **11/24/25 11:43:00 PM**

▼

Page 16: [85] Deleted **Rose Oelkers** **11/24/25 11:43:00 PM**

▼

Page 16: [86] Deleted **Rose Oelkers** **11/24/25 11:43:00 PM**

▼

Page 16: [86] Deleted **Rose Oelkers** **11/24/25 11:43:00 PM**

▼

Page 16: [86] Deleted **Rose Oelkers** **11/24/25 11:43:00 PM**

▼

Page 16: [86] Deleted **Rose Oelkers** **11/24/25 11:43:00 PM**

▼

Page 16: [86] Deleted **Rose Oelkers** **11/24/25 11:43:00 PM**

Page 20: [90] Deleted **Rose Oelkers** **11/24/25 11:43:00 PM**

▼

Page 20: [90] Deleted **Rose Oelkers** **11/24/25 11:43:00 PM**

▼

Page 20: [91] Deleted **Rose Oelkers** **11/24/25 11:43:00 PM**

▼

Page 20: [92] Deleted **Rose Oelkers** **11/24/25 11:43:00 PM**

▼

Page 20: [93] Deleted **Rose Oelkers** **11/24/25 11:43:00 PM**

▼

Page 20: [94] Deleted **Rose Oelkers** **11/24/25 11:43:00 PM**

▼

Page 20: [95] Deleted **Rose Oelkers** **11/24/25 11:43:00 PM**

▼

Page 20: [96] Deleted **Rose Oelkers** **11/24/25 11:43:00 PM**

▼

Page 20: [97] Deleted **Rose Oelkers** **11/24/25 11:43:00 PM**

▼

Page 20: [97] Deleted **Rose Oelkers** **11/24/25 11:43:00 PM**

▼

Page 20: [98] Deleted **Rose Oelkers** **11/24/25 11:43:00 PM**

▼

Page 20: [98] Deleted **Rose Oelkers** **11/24/25 11:43:00 PM**

▼

Page 20: [98] Deleted **Rose Oelkers** **11/24/25 11:43:00 PM**

▼

Page 20: [98] Deleted **Rose Oelkers** **11/24/25 11:43:00 PM**

▼

Page 20: [98] Deleted **Rose Oelkers** **11/24/25 11:43:00 PM**

▼

Page 20: [98] Deleted **Rose Oelkers** **11/24/25 11:43:00 PM**

